Master Thesis

Transient Multiphase Flow Analysis of Fluid Level Measurements

Abbas Zamani

1035390

Department of Mineral Resources & Petroleum Engineering

Chair of Petroleum and Geothermal Energy Recovery

Supervisor: Univ.-Prof. Dipl.-Ing. Dr.mont. Herbert Hofstätter

Leoben, 2014

EIDESSTATTLICHE ERKLÄRUNG

Ich erkläre hiermit an Eides statt, dass ich diese Arbeit selbständig, andere als die angegebenen Quellen und Hilfsmittel nicht benutzt und mich auch sonst keiner unerlaubter Hilfsmittel bedient habe.

AFFIDAVIT

I declare in lieu of oath, that i wrote this thesis and performed the associated research myself, using only literature cited in this volume.

_____ _____

Datum/Date Unterschrift/Signature

ACKNOWLEDGEMENT

First of all, I would like to show my gratitude to Univ.-Prof. Dipl.-Ing. Dr.mont. Herbert Hofstätter, for giving me the opportunity to work on my master thesis, and for his guidance and support from the initial stages of this project.

I am heartily grateful to DDipl. -Ing. Christian Burgistaller, my industrial supervisor at RAG company, for his continuous support, encouragement, and sharing his great experiences with me while working on this project.

I would like to extend my gratitude to Dr. Markus Kästenbauer, from RAG Company for his great advices.

I sincerely appreciate the great supports of Dr. Siroos Azizmohammadi, and Dr. Shaho Bazrafkan during my Master studies.

At last but not the least, I would thank my parents, Khatoun and Mohammad, Who always supported me, without which this work would be impossible.

ABSTRACT

Multiphase flow occurs during the production of oil and gas in the wellbores. Modelling and analyzing of this phenomenon is important for monitoring well productivity and designing surface facilities.

The ability to estimate and monitor the bottomhole pressure in pumping oil wells when multiphase flow is dominated plays an important role to provide viable information regarding both reservoir and artificial lift performance. Bottomhole pressure estimate becomes more complicated and maybe erroneous when transient multiphase flow conditions occur.

Transient multiphase flow in the wellbore causes problems in well test interpretation when the pump is shut off and the well is shut in at surface or sandface and the bottomhole pressure is estimated.

In this study, two numerical methods were presented to calculate bottomhole pressure using fluid level measurements by MURAG tool in two deviated pumping oil wells at steady state and transient condition.

In the first method, well models were built applying Prosper software, then bottomhole pressure was calculated using fluid level data in Excel employing various assumptions, definitions, and concepts especially for the part of the wellbore occupied with the oil and gas mixture called gaseous liquid column. Required fluid properties for calculations obtained from Prosper models.

The second presented method to calculate bottomhole pressure utilized Visual Basic programming in Excel to divide the wellbore annulus into 10-meter intervals. It was programmed to calculate pressure within each individual interval in Prosper using fluid level changes and considering some

assumptions. OpenServer was utilized to link the VB-Script (codes) to Prosper for calculations.

The outcome of this research led to accurate and reliable calculations of bottomhole pressure by comparing the results with the measured field data and well test interpretations.

Kurzfassung

Bei der Öl- und Gasproduktion tritt in den Fördersonden Mehrphasenfluss auf. Die Analyse und Modellierung dieses Phänomens ist für die Überwachung der Sondenproduktivität und die Auslegung von Obertageanlagen von Bedeutung.

Die Fähigkeit, den Bodenfließdruck in Ölfördersonden bei Mehrphasenfluss bestimmen zu können, liefert wertvolle Informationen zur Ermittlung von Lagerstättenparametern und der Effizienz der Förderausrüstung. Die Ermittlung des Bodenfließdruckes bei Mehrphasenfluss ist speziell für nicht stationäre (zeitabhängige) Bedingungen komplex. Die Interpretation von Sondentests, mit deren Hilfe der Bodenfließdruck nach Einschluss der Sonde ermittelt wird, wird durch das Auftreten von Mehrphasenfluss erschwert.

In dieser Studie werden zwei numerische Methoden zur Bestimmung des Bodenfließdruckes bei stationären und nicht stationären Bedingungen vorgestellt, welche Messungen des Flüssigkeitsspiegels im Ringraum von zwei Ölfördersonden als Eingangsdaten verwenden. Die Flüssigkeitsspiegel wurden dabei mit dem “MURAG-20” Spiegelmessgerät gemessen.

Bei der ersten Methode werden Bodenfließdrücke basierend auf Flüssigkeitsspiegeldaten in Excel berechnet, wobei für diese Berechnungen auch Eingangsdaten wie z.B. Flüssigkeitseigenschaften benötigt werden, die mithilfe der Software Prosper ermittelt wurden. Bei dieser Methode werden im Bereich der vergasten Flüssigkeitssäule spezielle Modellierungskonzepte angewandt.

Bei der zweiten Methode zur Berechnung des Bodenfließdruckes kommt ein Visual Basic Programm in Excel zur Anwendung, welches den Ringraum in 10-Meter Teufenintervalle unterteilt. Für jedes Teufenintervall wird der Druckgradient mittels PROPSER berechnet, wobei die OpenServer-Funktionalität von Prosper zum Datenaustausch mit dem Visual Basic Progamm herangezogen wird. Flüssigkeitsspiegeldaten werden auch bei dieser Methode als Eingangsdaten verwendet.

Die Ergebnisse dieser Berechnungsmethoden wurden mit gemessenen Felddaten und Ergebnissen von Sondentests verglichen. Das Resultat dieser Studie sind genaue und zuverlässige Berechnungen des Bodenfließdruckes in Ölfördersonden bei stationären und nicht stationären Fließverhältnissen.

Table of Contents

List of Figures

List of Tables

List of Abbreviations

AOF	Absolute Open Flow
g	Acceleration Owing to Gravity
D_a	Adjusted Fluid Level Depth
ρ	Density
w	Face Mass Flow Rate
q	Flow Rate
FL	Fluid Level
F	Friction Factor
$jt\ (s)$	Joint (s)
Z	Gas Compressibility Factor
R	Gas Constant
γ	Glowing Mass Fraction
H	Hold up
IPR	Inflow Performance Relationship
ID	Inner Diameter
σ	Interfacial Tension
MD	Measured Depth
OD	Outer Diameter
$PERF$	Perforation
P	Pressure
PG	Pressure Gradient
PI	Productivity Index
k	Ratio of Specific Heats

P_r	Reservoir Pressure
RAG	Rohöl Aufsuchungs AG
v_s	Slip Velocity
a	Speed of Sound in a Gaseous Medium
v_{sg}	Superficial Gas Velocity
v_{sl}	Superficial Liquid Velocity
T	Temperature
t	Time
TVD	True Vertical Depth
v	Velocity
μ	Viscosity
VB	Visual Basic
f	Void Fraction
WC	Water Cut
P_{wf}	Wellbore Flowing Pressure
TWM	Total Well Management

CHAPTER 1: INTRODUCTION

A large fraction of the energy consumed in the world comes from hydrocarbon reserves in the earth. These reserves are finite and should be produced efficiently. The hydrocarbon mixture is generally produced through wells drilled into the reservoir pay zones. During oil production, multiphase flow commonly occurs in different sections of a flow-line such as the wellbore, the tubing, the casing/tubing annulus, and the surface equipment. Despite vast research efforts in this area, the complexity of multiphase flow combined with other processes still remains a challenging problem.

During production, pressure declines in the reservoir due to fluid withdrawal. Pressure also decreases in the wellbore when fluid moves from the bottomhole to the wellhead. Typically, gas liberates from the oil phase if the pressure becomes less than the bubble point in the reservoir or wellbore. Water is often produced with the hydrocarbon mixture. Hence, we expect multiphase flow in some sections of the wellbore.

Successful oil field development requires reliable information about reservoir conditions such as reservoir permeability, near wellbore damage, reservoir pressure, drainage area, reservoir faults and boundaries. Many of these parameters are obtained through geological studies, core examination, well logs and pressure transient tests.

During a pressure transient test, fluid flow rate is changed and the pressure response due to the flow rate change is measured at the well. The recorded data are then analyzed to estimate reservoir properties and completion efficiency. Pressure transient tests are performed in a variety of forms. One major type is a buildup test, which is performed by measurement

and analysis of the bottomhole pressure. After the well has been produced for a period of time at a constant rate, a pressure buildup test can be conducted by recording the bottomhole pressure responses when the well is shut in at the surface or sandface.

When an oil well is shut in, phase segregation may occur along the wellbore. This phase segregation takes place due to the differences between gas, oil and water densities. The gas phase moves upward while the liquid phase moves to the lower section of the well due to gravity. This segregation affects the interpretation of the well testing analysis and the reliability of the measured data in the wellbore.

After shutting in an oil well, three regions are formed along the casing/tubing annulus including a continuous gas phase region, a region which is occupied by an oil column and finally a water region. When an oil reservoir is producing from a gas cap and/or below the bubble point pressure, free gas is entering the wellbore accompany with liquids. As the pressure reduces along the wellbore, the solution gas in oil is released. The more pressure decline, the more gas is released from the oil column. In the oil column, when gas is present, vented through or in solution, a gaseous oil column is formed. The depth to this gas lightened oil column can be measured using different fluid level measurement techniques.

Bottomhole pressure calculation is required to get a good insight of well and reservoir performances during production when steady state is dominated and after shutting in a well and initiating build-up test when transient condition is dominated. Calculation of pressure increase across the gas column is straightforward, but uncertainty arises in the oil column when gas is present.

In the following sections, first, the Company will be introduced briefly, then, the scope of this study and the main objectives pursued and achieved in this research will be discussed. In addition, the structure and the different chapters of the thesis in the following sections will be introduced.

1.1 Company Background

Rohöl-Aufsuchungs Aktiengesellschaft (RAG) is Austria's oldest oil and gas Company. Its core areas of business are oil and natural gas exploration and production, and gas storage. A joint venture between RAG, Gazprom and Wingas operates the Haidach gas storage facility, and another, with E.ON Gas Storage, runs the seven Fields storage facility. Both facilities straddle the border between the provinces of Salzburg and Upper Austria.

Through its own storage capacity and its role as an operator, RAG plays an important part in the security of supply for Austria and the whole of Central Europe. The storage capacity now totals 5 billion cubic meters, and a further billion cubic meters will be added by 2014. The activities also include crude oil stockpiling, natural gas trading and transportation, and renewable energy projects.

Since its foundation RAG has produced over 15 million tons of crude oil and 24.5 billion cubic meters of natural gas. In the past few years RAG has added to its exploration and production acreage, and its operations now extend to Germany, Hungary, Poland, and Romania.

1.2 Statement of the Problem

- To analyze the multiphase flow in two wells using fluid level measurement data.

- To select the best software package to suit the research`s analysis and modelling.
- To calculate bottomhole pressure at steady state and transient condition. (the focus is on transient condition)
- To investigate the applicability of the S-Curve method, proposed by Podio et. al. [28].
- Can black oil approach be helpful? If yes, how?

- To assess the accuracy of the proposed methods by comparing the calculated bottomhole pressure with the bottomhole pressure measured by the downhole pressure gauges.

1.3 Research Objectives

Through this study, the researcher aims to investigate the Transient Multiphase Flow Analysis of Fluid Level Measurements. During this study a Literature review on multiphase flow models (including software packages) describing the transient period of fluid level changes in oil and gas wells will be carried out. Various fluid level measuring techniques are considered. The next step will be dedicated to the modeling of bottomhole pressure (including pressure buildup curves) from dynamic fluid level measurements. Comparison of calculated bottomhole pressure from dynamic fluid level data with downhole pressure measurements is the last part of this study.

Following is a list of questions that the researcher seeks for answers throughout this study:

- Which software package better suits the requirements for modeling and analysis of the transient multiphase flow case?

- How can the S-curve method be applied in the current case?
- Which fluid level measuring techniques can give the best input data to calculate bottomhole pressure?
- Are calculated buttomhole pressures from dynamic fluid level data in a good agreement with bottomhole pressure measured by downhole gauges?

1.4 Brief Description of the Chapters

In chapter 2, the methods, correlations, concepts, techniques and literature associated with the bottomhole pressure calculation will be described. In chapter 3, the methods employed for bottomhole pressure calculation will be discussed in detail. In that chapter all the assumptions made and the correlations used coupled with the logics behind them beside other necessary information will be explained. Chapter 4 will be dedicated to the results of the employed methods and the comparison of them with the real values coupled with the interpretation of the results and comparisons. Finally, chapter 5 will present the conclusion of the discussed methods and results and the whole thesis. At the end, some recommendations will be given for further work.

CHAPTER 2: LITERATURE REVIEW AND THEORY

2.1 Multiphase Flow Modeling In Wellbores

Multiphase flow is commonly encountered during oil production, and has a strong impact on the performance of reservoir and surface facilities. Multiphase flow may occur in different sections of the flow path such as in the wellbore, the tubing, the casing/tubing annulus, and surface equipment. The frequent occurrence of multiphase flow in petroleum industry emphasizes the challenge of analyzing and modeling multiphase systems to optimize the performance of wells or reservoirs coupled to surface facilities. Since the last couple of decades, complex drilling and completion methods, such as those applied to multilateral and horizontal wells, have added new challenges for realistic reservoir modeling.

Parameters, such as pressure, temperature, velocities and phase fractions, must be modeled in production operations. When co-current flows of multiple phases occur, the interface between phases can take on a variety of configurations, known as flow patterns [7]. The particular flow pattern depends on the conditions of pressure, flow, and channel geometry and is a very important feature of two-phase flow [19]. The hydrodynamics of the flow and the flow mechanisms change significantly from one flow pattern to another. To accurately estimate the pressure drop and phase fraction, it is necessary to know the flow pattern (or regime) for any flow conditions. These patterns include bubble, slug, churn, annular and mist flow for vertical multiphase flow. (Flow patterns will be discussed in the next section of this chapter.)

A large range of different pressure gradient correlations are published. In addition, many methods and correlations developed are kept confidential.

As stated by Time (2009) [34]; “There is no guarantee that the correlations kept confidential are better than other correlations. On the contrary, keeping methods secret is a way to avoid scientific testing, and the methods may have low validity.”

One may divide the pressure gradient calculations into two categories:

1) Empirical correlations, based on experimental data and dimensional analysis.

2) Mechanistic correlations, based on simplified mechanistic (physical) considerations like conservation of mass and energy.

It can be quite difficult to discriminate between empirical and mechanistic correlations. Often a combination is used to develop multiphase correlations [37].

The empirical correlations are generated by establishing mathematical relations based on experimental data. Dimensional analysis is often used to select correlating variables. It is important to notice that application of empirical correlations is limited to the range of data used when it was developed [10], [37]. Further it is possible to divide the empirical correlations in groups regarding if slip and flow patterns are considered, see table 2.1.

Over the past few years, a number of numerical and analytical wellbore simulators have been developed for multiphase and single-phase flow in the wellbores. The simplest approaches to compute multiphase flow variables in the wellbore employing simulators are using empirical correlations.

The mechanistic correlations are based on a phenomenological approach and they take into account basic principles, like conservation of mass and energy [37]. In mechanistic models, flow Pattern determination is

important. “Normally” a mechanistic transport equation is written for each of the phases in the multiphase flow. Separate models for predicting pressure drop, liquid holdup and temperature profile have been developed by flow Pattern determination and separating the phases [10].

Table 2.1: Classification of correlations

Correlation	Category	Slip Considered?	Flow Pattern Considered?
Farncher & Brown	Empirical	No	No
Gray	Empirical	Yes	No
Hagedorn & Brown	Empirical	Yes	No
Duns & Ros	Empirical	Yes	Yes
Orkiszewski	Empirical	Yes	Yes
Beggs & Brill	Empirical	Yes	Yes
Mukherjee & Brill	Empirical	Yes	Yes
Petroleum Experts (1,2,3)	Empirical	Yes	Yes
Petroleum Experts (4,5)	Mechanistic	Yes	Yes
Hydro 3-Phase	Mechanistic	Yes	Yes
OLGAS	Mechanistic	Yes	Yes

The main difference between the empirical correlations is how liquid holdup, mixture density and friction factors are estimated. The correlations defined as empirical in table 2.1 will be described in the following sections.

2.1.1 Fancher and Brown Correlation [11]

Is a no-slip hold-up correlation that is provided for use as a quality control. It gives the lowest possible value of VLP since it neglects gas/liquid

slip it should always predict a pressure which is less than the measured value. Even if it gives a good match to measured downhole pressures, Fancher Brown should not be used for quantitative work. Measured data falling to the left of Fancher Brown on the correlation comparison plot indicates a problem with fluid density (i.e PVT) or field pressure data.

2.1.2 Gray Correlation [15]

Gray developed an empirical correlation for a vertical well producing gas and gas condensate or water. Slip is considered, but it does not distinguish between different flow patterns, see table 2.1. Gray cautioned use of the correlation beyond the following limits:

- velocities higher than 50 ft/sec
- nominal diameters larger than 3.5 in
- condensate or liquid loadings above 50 bbl/MMscf
- water or liquid loadings above 5 bbl/MMscf

2.1.3 Hagedorn and Brown Correlation [16]

Performs well in oil wells for slug flow at moderate to high production rates (well loading is poorly predicted). Hagedorn and Brown correlation should not be used for condensates and whenever mist flow is the main flow pattern. It under predicts VLP at low rates and should not be used for predicting minimum stable rates.

2.1.4 Duns and Ros Correlation [9]

The Duns and Ros method is an empirical correlation based on approximately 4000 two-phase flow experiments. In the Duns and Ros correlation it is discriminated between three main flow regimes. Liquid holdup and friction factor correlations were developed for each flow regime.

The Duns and Ros correlation discriminates between three different flow regimes. These are shown in figure 2.1, described as regions. Where N_{LV} and N_{GV} are dimensionless liquid velocity number and dimensionless gas velocity number respectively. In region I, liquid is the continuous phase. Where gas and liquid phase's alternate is referred to as region II and in region III gas is the continuous phase. A transition pattern is treated as a fourth pattern in calculations. For flow in the transition regions linear interpolation may be used to approximate the pressure gradient.

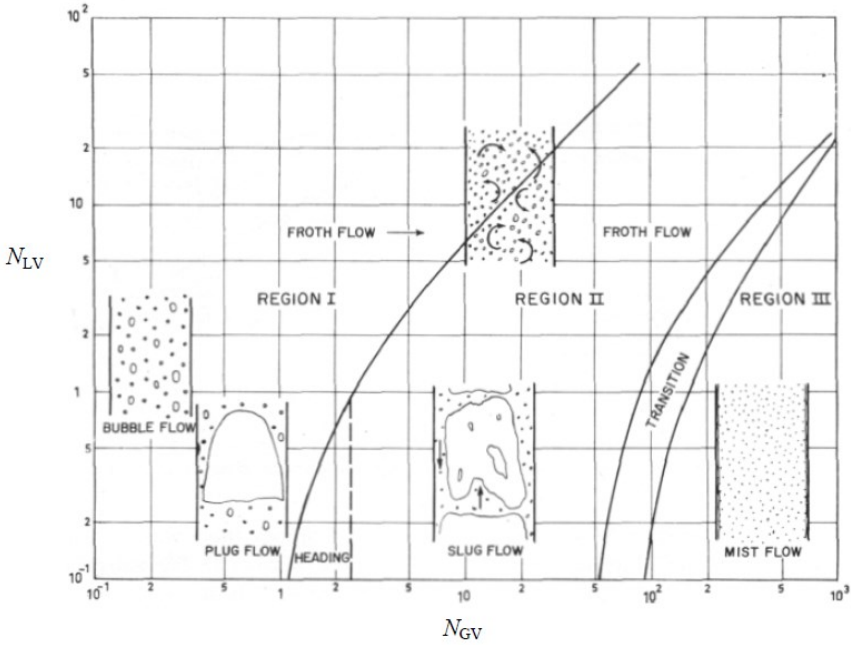

Figure 2.1: Flow regime map [9]

This correlation performs well in mist flow cases and may be used in high GOR oil wells and condensate wells.

2.1.5 Orkiszewski Correlation [25]

Orkiszewski compared many of the published correlations against test data. He concluded that none of them sufficiently described two phase flow for all the flow regimes. Thereby a combination of the correlations that best described the test data was suggested to be used. Orkiszewski uses Griffith

and Wallis method for slug flow, Duns and Ros for transition and mist flow, and he suggested a new method for slug flow.

This correlation often gives a good match to measured data. However, its formulation includes a discontinuity at velocity equal to 10 $(\frac{ft}{\sec})$ in its calculation method. The discontinuity can cause instability during the pressure matching process.

2.1.6 Beggs and Brill Correlation [1]

This correlation is primarily a pipeline correlation. It generally over predicts pressure gradients in vertical and deviated wells.

2.1.7 Petroleum Experts' Correlations [26]

Petroleum Experts correlations are a combination of different correlations. It is developed by the company Petroleum Experts. Flow regimes are determined using Gould et al. (1974) [13] flow map. See table 2.6 for correlations used in the various flow regimes. Liquid holdup and frictional factors are found using the respective flow correlations.

Table 2.2: Correlations used by Petroleum Experts Correlation

Flow Regime	Correlation
Bubble Flow	Wallis and Griffith
Slug Flow	Hagedorn and Brown
Transition	Duns and Ros
Annular Mist Flow	Duns and Ros

2.2 Multiphase Flow Basic Parameters

Multiphase flow is complicated because at each section of the wellbore multiple phases are simultaneously competing for the available cross-

sectional area. Computing each phase fraction is very important for determining the pressure gradient in multiphase flow. The basic governing equation used to calculate the pressure drop in a steady state condition is the momentum equation:

$$\frac{dP}{dz} = -(\rho_m v_m \frac{dv_m}{dz} + \rho_m g \sin\theta + \frac{2\rho_m f_m v_m^{\,2}}{d}) \tag{2.1}$$

Where P is the pressure in the wellbore and v_m, ρ_m and f_m represent mixture properties for velocity, density, and friction factor. On the right side of equation 2.1, the first term, $\rho_m v_m \frac{dv_m}{dz}$ shows the momentum flux. The second term $\rho_m g \sin\theta$ is the body force due to gravity. The last term, $\frac{2\rho_m f_m v_m^{\,2}}{d}$ represents the momentum losses due to friction. Hence, we can rewrite the steady state pressure gradient as a combination of kinetic energy, $(\frac{dP}{dz})_A$, static head , $(\frac{dP}{dz})_H$, and friction gradient, $(\frac{dP}{dz})_F$.

$$(\frac{dP}{dz}) = (\frac{dP}{dz})_A + (\frac{dP}{dz})_H + (\frac{dP}{dz})_F \tag{2.2}$$

Equation 2.1 shows that we need mixture parameters, such as mixture density, to calculate pressure change in wellbores. Mixture parameters depend directly on in-situ volume fractions of the phases. For example, in a two-phase gas and oil system, the mixture density and viscosity are related to the in-situ liquid volume fraction (holdup), H , as follows:

$$\rho_m = \rho_l H + \rho_g (1 - H) \tag{2.3-a}$$

$$\mu_m = \mu_l H + \mu_g (1 - H) \tag{2.3-b}$$

The in-situ fraction of a phase is generally different from its input fraction. The main reason for this is the differences between gas and liquid velocities caused by their density differences. Thus, a major effort in modeling multiphase-flow is the correct estimation of in-situ phase volume fraction. In this section we discuss some definitions that are used in multiphase flow. In the next section we present different models to compute phase fractions in the wellbore.

2.2.1 Flow Patterns

Single-phase flow is divided into laminar and turbulent flow regimes depending on their Reynolds numbers. In multiphase flow the discrimination becomes more complex. Gas and liquid distribution may vary when flowing in a long pipe, resulting in different flow regimes [34]. A brief description of the flow regimes or patterns that may occur in vertical or horizontal flow will be given in this section.

In general one may discriminate between five flow regimes for vertical upward multiphase flow: bubble flow, slug flow, churn flow, annular and mist flow, see figure 2.2. The flow regimes change in this order by increasing gas rate for a given liquid rate [38]. The most important flow patterns for multiphase flow in wells are slug and churn flow patterns. They are often referred to as intermittent flow regimes [3]. Mist flow and annular-mist flow are other names for the annular flow regime [4].

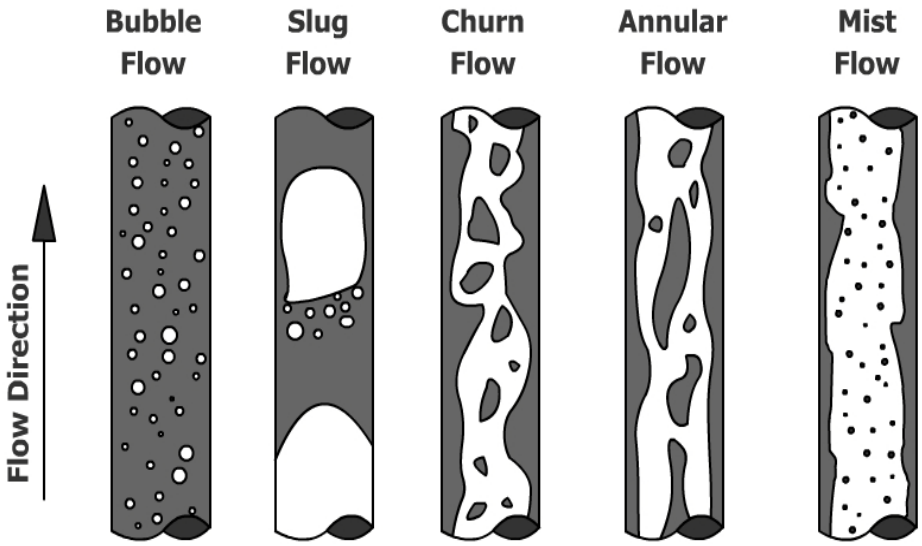

Figure 2.2: Flow patterns for upward vertical flow [3]

2.2.1.1 Bubble Flow

In bubble flow, liquid is the continuous phase and the free-gas phase is presented as small bubbles. The gas-bubbles are randomly distributed in the liquid flow, and the diameter may vary. Due to different sizes of the gas-bubbles, they travel with different velocities. The liquid phase however moves with a more uniform velocity. The gas phase, except for its density, has little effect on the pressure drop [25].

2.2.1.2 Slug Flow

Slug flow is characterized by alternating slugs of liquid with large bubbles of gas. Large gas-bubbles are made as the smaller gas-bubbles coalesce, when gas velocity increases. The larger bubbles are called Taylor bubbles. Smaller bubbles of gas are contained in the liquid slugs. Liquid is still the continuous phase, because of a liquid film covering the Taylor bubbles [38].

2.2.1.3 Churn Flow

As the gas velocity is increased further, the large gas-bubbles become unstable and may collapse. When this happens, churn flow occur. Churn flow is a highly turbulent and chaotic regime. Neither gas nor liquid phase appears to be continuous. Oscillatory, up and down motion of liquid, is characteristic for churn flow [38].

2.2.1.4 Annular Flow

In annular flow, gas is the continuous phase. Gas flows with a high rate in the centre of the pipe. Liquid is found as a liquid film coating the pipe wall and as entrained droplets in the gas phase. The gas phase becomes the controlling phase [25].

2.2.1.5 Mist Flow

The gas phase is continuous, and the bulk of the liquid is entrained as droplets in the gas phase.

Determination of flow regime will be important for parameters such as holdup and thereby pressure-drop predictions. Results of studies on flow regimes are often displayed in the form of a flow regime map [2]. Flow maps are generated to relate flow patterns to flow rates and fluid properties. Boundaries in a flow regime map represents where a regime becomes unstable. A growth of the instability will lead to transition to another regime. These transitions can be rather unpredictable because they may depend on otherwise minor features of the flow, as the wall roughness or entrance conditions. Hence, the flow-pattern boundaries are not distinctive lines, but more poorly defined transition zones. Many different flow regime maps have been published, based on different correlations for flow-regime prediction.

Most of them are dimensionless and apply only for the specific pipe size and fluids used when they were created [2] [38].

2.2.2 Superficial Velocities

Superficial velocity of any phase is its velocity if we assume that it occupies 100% of the cross section of the pipe. Thus, the superficial velocity for liquid phase, v_{sl}, is given in terms of the in-situ volumetric flow rate of liquid phase, q_l and the cross- sectional area, A by equation 2.4.

$$v_{sl} = \frac{q_l}{A} \tag{2.4}$$

A similar equation is valid for the gas phase, so its superficial velocity is a function of cross sectional area and the in-situ gas flow rate, q_g as:

$$v_{sg} = \frac{q_g}{A} \tag{2.5}$$

Since during two-phase flow none of the phases occupies the entire cross- sectional area, the available area for each phase is less than A , and the actual velocity of each phase is higher than the superficial velocity.

2.2.3 Volume Fraction, Mass Fraction

Since multiphase flow contains more than one phase we need to know the relative amount of each phase in each section of the wellbore. We can express this value either as a volume fraction or as a mass fraction. The liquid volume fraction, f_l, is the fraction of volumetric flow rate of liquid divided by the total flow rate of the mixture.

$$f_l = \frac{q_l}{q_t} = \frac{q_l}{q_l + q_g} = \frac{v_{sl}}{v_{sl} + v_{sg}} \tag{2.6}$$

Similarly, the gas volume fraction is the volumetric flow rate of gas divided by the total flow rate of the mixture.

$$f_g = \frac{q_g}{q_t} = \frac{q_g}{q_l + q_g} = \frac{v_{sg}}{v_{sl} + v_{sg}} \tag{2.7}$$

The flowing gas mass fraction, γ_g, is defined in terms of the mass flow rates of the liquid phase (w_l) and gas phase (w_g) as:

$$\gamma_g = \frac{w_g}{w_t} = \frac{w_g}{w_g + w_l} = \frac{v_{sg}\rho_g}{v_{sg}\rho_g + v_{sl}\rho_l} \tag{2.8}$$

Similarly, the flowing liquid mass fraction, γ_l, is defined as:

$$\gamma_l = \frac{w_l}{w_t} = \frac{w_l}{w_g + w_l} = \frac{v_{sl}\rho_l}{v_{sg}\rho_g + v_{sl}\rho_l} \tag{2.9}$$

From equations 2.8 and 2.9

$$\gamma_g + \gamma_l = 1 \tag{2.10}$$

The void fraction of gas in the mixture (in-situ gas volume fraction) (f_g) is defined as the ratio of the total cross sectional area through which the gas flows, A_g and the total cross sectional area A.

$$f_g = \frac{A_g}{A} \tag{2.11}$$

Since gas flows only through A_g, the actual velocity of gas phase is expressed as $\frac{q_g}{A_g}$. From equation 2.5 the actual velocity of the gas phase can be written as:

$$v_g = \frac{v_{sg}}{f_g} \tag{2.12}$$

Similarly, we can define the in-situ fraction of liquid in the mixture, f_l, which is also called holdup, H . Normally, the liquid flows more slowly than the gas and accumulates in the pipe section.

$$H = f_l = \frac{A_l}{A} = 1 - f_g \tag{2.13}$$

Where A and A_l are the total cross sectional area and the available area for liquid movement respectively. Figure 2.3 shows a schematic of liquid and gas fraction definition. Similar to equation 2.12, the actual liquid velocity is defined as:

$$v_l = \frac{v_{sl}}{f_l} \tag{2.14}$$

The total velocity of the mixture v_m is defined as:

$$v_m = v_{sl} + v_{sg} \tag{2.15}$$

Combining equations 2.12 through 2.15 the mixture velocity can be rewritten as:

$$v_m = Hv_l + (1-H)v_g \tag{2.16}$$

The velocities of phases depend on fluid gravity, so in a vertical wellbore the lighter phase moves faster than the heavier phase. The difference between the velocities is denoted as slip velocity, v_s :

$$v_s = v_g - v_l = \frac{v_{sg}}{1-H} - \frac{v_{sl}}{H} \tag{2.17}$$

2.3 Flow Regimes Categories

At different times, fluid flows in the reservoir with different ways generally based on the shape and size of the reservoir. Flow behavior classification is studied in terms of pressure rate of change with respect to

time. Three main flow regimes will be described in this sub-chapter; they are steady-state flow, pseudo steady state flow, and transient state flow.

2.3.1 Steady State Flow

In steady state flow, there is no pressure change anywhere with time (equation 2.18). It occurs during the late time region when the reservoir has gas cap or aquifer support. This condition is also called constant pressure boundary in which pressure maintenance might apply in the producing formation.

$$\frac{\partial p}{\partial t} = 0 \tag{2.18}$$

2.3.2 Pseudo Steady State Flow

This flow regime also occurs in late-time region, but it forms when there is no flow in the reservoir outer boundaries. No flow boundaries can be caused by the effect of nearby producing wells or presence of sealing faults. It is a closed system or acts as a tank where a constant rate production results in constant pressure drop for each unit of time (equation 2.19). This flow is also called semi-steady state or depletion state.

$$\frac{\partial p}{\partial t} = \text{constant} \tag{2.19}$$

2.3.3 Transient Condition Flow

When the pressure/rate changes with time due to well geometry and the reservoir properties (i.e. permeability and heterogeneity), it indicates that transient (unsteady state) flow occurs (equation 2.20). It is observed before boundary effects are reached or also called infinite acting time period. Higher

compressibility of the fluid leads to a more pronounced unsteady state effect of the reservoir fluid [6].

$$\frac{\partial p}{\partial t} = f(x, y, z, t) \tag{2.20}$$

2.4 Reservoir Inflow Performance

The Inflow Performance Relationship (IPR) is routinely measured using bottomhole pressure gauges at regular intervals as part of the field monitoring program. This relationship between flow rate (q) and wellbore flowing pressure (P_{wf}) is one of the major building blocks for a nodal-type analysis of well performance.

2.4.1 Single Phase Oil Flow IPR

Field measurements have shown that wells producing undersaturated oil (no gas at the wellbore) or water have a straight line IPR (Figure 2.3).

$$PI = \frac{q}{P_r - P_{wf}} \tag{2.21}$$

Where q is the flow rate and PI the Productivity Index, i.e. the well inflow rate per unit of well drawdown.

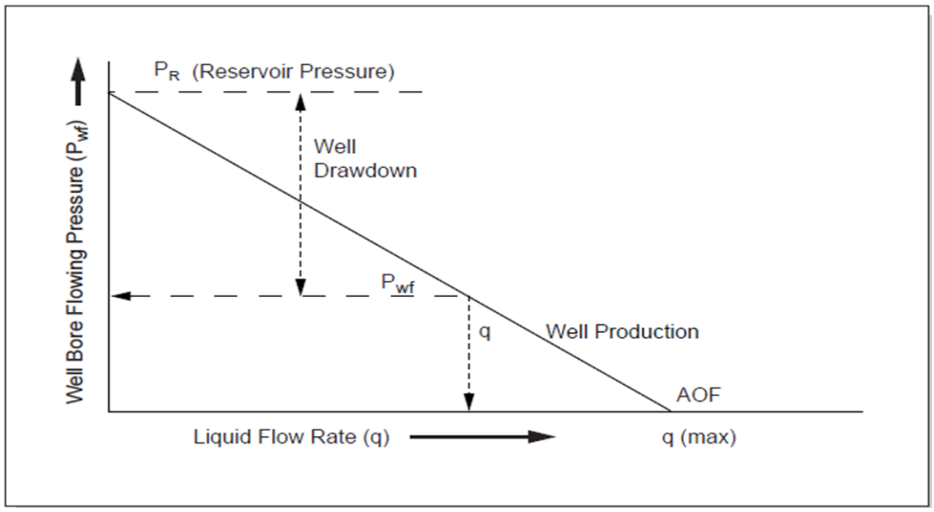

Figure 2.3: Straight line IPR (for an incompressible liquid) [28]

2.4.2 Productivity Index

The productivity index is used to define the productivity of a well and is dependent on the drawdown. The drawdown is the difference between the average reservoir pressure and the pressure at the perforation. This drawdown is a pressure drop and causes the production flow into the well from the producing formation. It is not constant but varies with production rate or pressure drawdown. In other words, it can be expressed; the more drawdown, the higher the production. The formula of the productivity index is mentioned below.

$$PI = \frac{q}{(P_r - P_{wf})} \tag{2.22}$$

2.4.3 Two-Phase Flow IPR

The compressible nature of gas results in the IPR is no longer being a straight line. Straight line IPR is also not applicable to when two phase inflow is taking place, e.g. when saturated oil is being produced. Vogel (1968) [35] proposed the following equation based on a large number of well performance simulations:

$$\frac{q}{q_{\max}} = 1 - 0.2(\frac{P_{wf}}{P_r}) - 0.8(\frac{P_{wf}}{P_r})^2 \tag{2.23}$$

Where $q_{\max}$ is the AOF, i.e. q when $P_{wf} = 0$.

Vogel's key contribution was the introduction of the concept of normalizing the production rate to the AOF value $(q_{\max})$. Rewriting equation 2.23 in this manner gives:

$$\frac{q}{q_{\max}} = \left\{1 - (\frac{P_{wf}}{P_r})^2\right\}^n \tag{2.24}$$

Which is virtually equivalent to Vogel's equation when $n = 1$ [12]. For example:

$$\frac{q}{q_{\max}} = 1 - (\frac{P_{wf}}{P_r})^2 \tag{2.25}$$

Figure (2.4) compares the production rate as a function of drawdown for an undersaturated oil (straight line IPR, line A) and a saturated oil showing the two phase flow effects discussed above (curve B). The figure also shows the special case (curve C) when the wellbore pressure is below the bubble point while the reservoir pressure is above, i.e. (incompressible) liquid flow is occurring in the bulk of the reservoir.

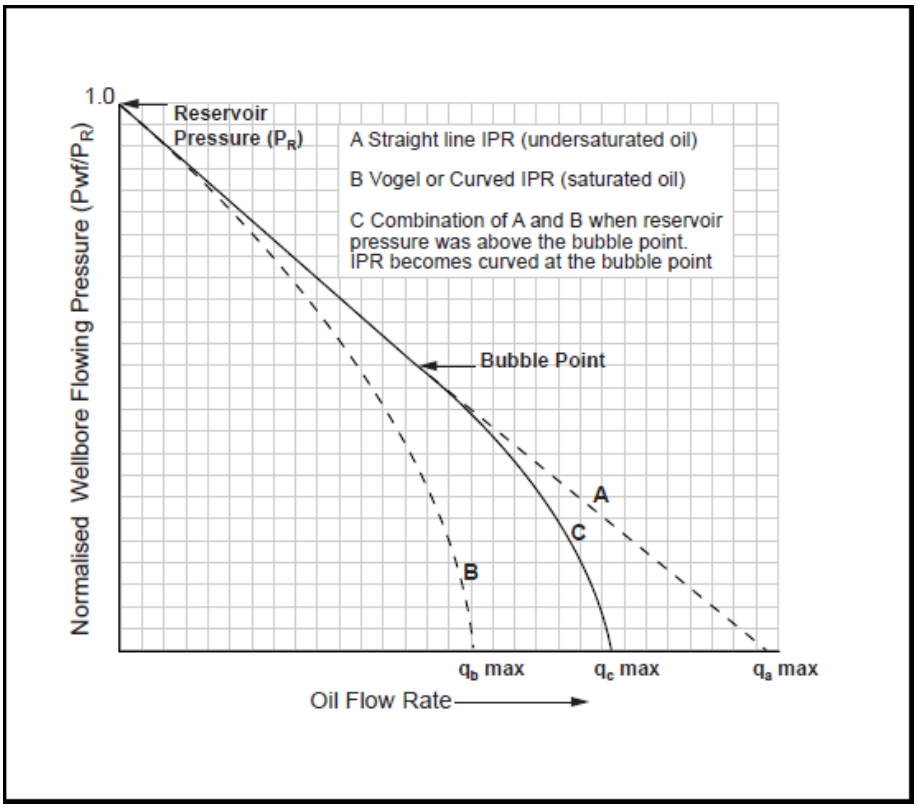

Figure 2.4: Inflow Performance Relationships [28]

2.5 Well Testing

A transient pressure test is a fluid-flow test conducted on wells to obtain reservoir and well completion data. During the test, the well's flow rate is changed and the well's pressure response as a function of time is

measured at the same well or at other neighboring wells. The pressure response is a function of reservoir rock properties, fluid properties completion efficiency and flow geometry. Based on the well type (injector or producer) and flow rate (producing or shut in) several kinds of tests may be designed.

The most common well test type is the pressure buildup test. This test is conducted on a well which has been producing at a constant rate and is then shut in at the surface or sandface. A pressure recorder is lowered into the well to record the pressure in the wellbore for several hours, depending on the anticipated formation permeability. The pressure may be measured opposite the producing zone near the formation or at other parts of the wellbore. If the recorder is located far from the perforation zones, the measured pressure should be converted to sandface pressure, which is then analyzed to estimate formation permeability, skin factor, average reservoir pressure, distance to a fault if present, fracture length and fracture conductivity.

It is important to be certain that the measured data are not affected by the wellbore dynamics due to wellbore storage and phase redistribution when more than one phase is flowing simultaneously in the wellbore.

Most well tests are performed by changing the flow rate at the surface, rather than at the bottomhole in order to minimize costs. For example, during a buildup test, the well is shut in at the surface not at the bottomhole, hence, fluid influx from the reservoir is allowed to flow into the wellbore after shut in. This phenomenon, whereby the change in sandface flow rate lags behind the surface flow rate change, has been called wellbore storage, which dominates the initial pressure response. To use this period in well testing interpretation, it

is necessary to detect the presence and duration of wellbore storage in early transient pressure data. In the effort to quantify and evaluate the wellbore related effects, the concept of wellbore storage is followed by the concept of phase redistribution phenomena [30].

Wellbore phase redistribution occurs in a shut-in well with gas and liquid flowing simultaneously in the tubing. In such wells, the gravity effects cause the liquid to fall to the bottom and the gas to rise to the top of the tubing. Due to the relative incompressibility of the liquid and the inability of the gas to expand in a closed system, phase segregation yields a net increase in the wellbore pressure [29]. The increased pressure in the wellbore is then relieved to the formation and equilibrium occurs between the wellbore and the adjacent formation.

2.6 Fluid Level Measurement Techniques

Analyzing well performance is an important step toward increasing profits by improving production techniques. Periodic production tests, monitoring with Pump Off Controllers, dynamometer surveys, and fluid level measurements are the principal tools. Fluid levels are often the most cost effective way of monitoring the well.

Fluid level is an indirect indicator of wellbore pressure and could be important because it is involved in so many relationships.

Because of the importance of fluid level measurement as a surveillance tool, improving and extending the art and science of making fluid level measurement has been always a field of investigation.

Liquid levels may be detected using acoustic devices. Acoustic devices are popular because they are easy to operate, and the depth to the liquid level may be estimated from a visual inspection of the acoustic record.

The interpretation of liquid level data depends on wellbore mechanics and fluid properties. Ideally, the distance to the liquid level is calculated from a well-defined acoustic record by summing the number of couplings with their corresponding lengths. Typically, all pipe sections are not clearly delineated on an acoustic record. The liquid level distance is then obtained by integrating the relationship between acoustic velocity and time.

The presence of foam or obstructions may preclude using acoustic devices to detect liquid levels. The principal of mass balance of the gas phase in the annulus is employed to provide reasonable estimates of liquid level distances for these conditions. Annular gas volumes may be calculated from a mass balance technique using pressure transient data measured at the casing annulus. The distance to the liquid level is then calculated from the gas volume.

Another fluid level measurement tool called MURAG-20 was developed and presented by RAG Company in Austria, 2010. It is a fully automated fluid level measurement tool whose unique feature is its purely electronic functioning. The measuring device is enclosed, mounted on the casing valve and operates with zero emissions on the environment (no outlet of casing gas). The MURAG-20 device has a sampling rate of down to one measurement per minute.

2.6.1 Acoustic Devices

Liquid levels are determined using acoustic devices by generating a pressure pulse in the casing annulus or tubing at the surface. The pressure wave travels down the annulus and hits the liquid level which reflects the wave back to the surface. The pressure pulse is reflected by obstructions such as tubing collars or liner tops. Controlling the source of the pressure pulse has recently improved resolution in differentiating between types of reflections.

The measurement system and its components are shown in figure 2.5. This figure shows that the measurement system developed by Echometer Company is comprised of different parts such as computer, well analyzer, cables, sensors, and gas gun.

Figure 2.5: Portable well analyzer with sensors [36]

2.6.1.1 Measurement Technique

A gas gun is a conventional source of the pressure pulse due to the ease of storage, safety, simplicity, and economics. A gas gun is shown in figure 2.6 in details. The firing of a gas gun produces a powerful pressure

wave where vibrations may reduce the resolution of the detected signal. However, in a clean, single string of casing, a gas gun produces signals that are sufficiently interpretable [31].

The need for a better source pulse led to the development of the gas gun. On wells with less than 100 psi casing annulus pressure, the gas gun volume chamber is pressurized to approximately 100 psi greater than the annulus pressure. The sudden release of pressure creates a compressional pressure wave with a magnitude proportional to the pressure differential between the gas gun chamber and the wellbore. It is called explosion pulse. If the gas gun pressure is greater than 100 psi, the pressure path is reversed. A valve is opened to allow a sudden expansion of wellhead pressure into the gas chamber, creating a rarefaction pressure wave which is called implosion pulse [23].

The detected pressure pulse deforms piezoelectric material located in the receiver housing which releases an electrical pulse. The amplitude of the electric signal is proportional to the rate of deformation (strain) of the piezoelectric material. The electrical signal is then amplified, filtered, and recorded on a strip chart. Direct measurements are taken from the strip chart to determine acoustic travel time and liquid level distances.

Gas gun and its different parts are shown in figure 2.6. Figure 2.7 shows a gas gun attached to a well.

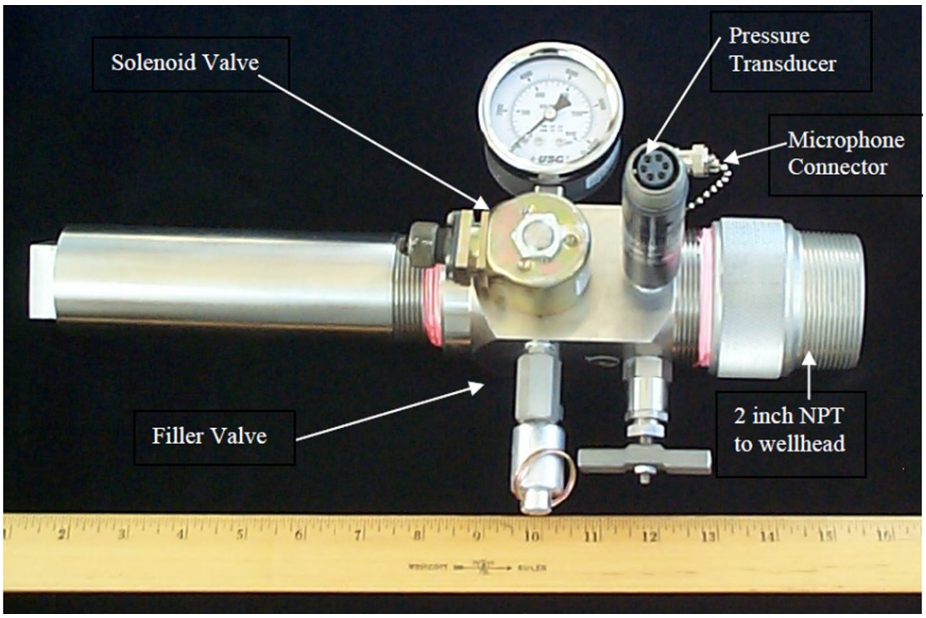

Figure 2.6: Gas gun and its different components [36]


Figure 2.7: Gas gun installed on a well [36]

2.6.1.2 Acoustic Determination of Liquid Levels

A well-defined acoustic record is shown in Figure 2.8. Here time and pressure pulse amplitude are recorded along the horizontal and vertical axes. The time between pulse generation and surface reflection is measured directly from the acoustic record. Only qualitative judgments can be made concerning the amplitude of the recorded signals. However, the size of deflection is used to differentiate between collars, liners and the liquid level.

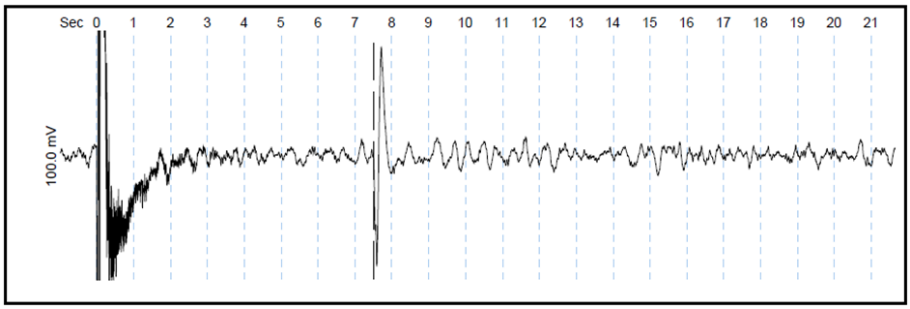

Figure 2.8: Example of an acoustic response of fluid level in a wellbore

2.6.1.3 Collar Summation Method

If tubing collar reflections are well defined on acoustic records, the liquid level depth is obtained by summing the number of pipe sections with their corresponding lengths. This technique is applicable to the acoustic record presented in Figure 2.9. Figure 2.9 indicates how the collars are shown in TWM software to measure fluid level. The collar summation may be carried out automatically or manually. Vertical tick marks are drawn to each individual collar reflection as they are counted. The collar display on this chart is obtained by digitally filtering the acoustic data at the precise collar frequency previously determined and shown on the depth determination tab in the lower left hand corner. The collar count is continued until the signal to noise ratio decreases below a preset limit. The average collar frequency $(\frac{jts}{\sec})$ is multiplied by twice the average joint length $(\frac{ft}{jt})$, entered in wellbore tab of the well file, to calculate the acoustic velocity in $(\frac{ft}{\sec})$. All pipe sections are not always interpretable, but a definite time interval exists. The time interval on the acoustic record can be used as the yardstick to calculate the liquid level.

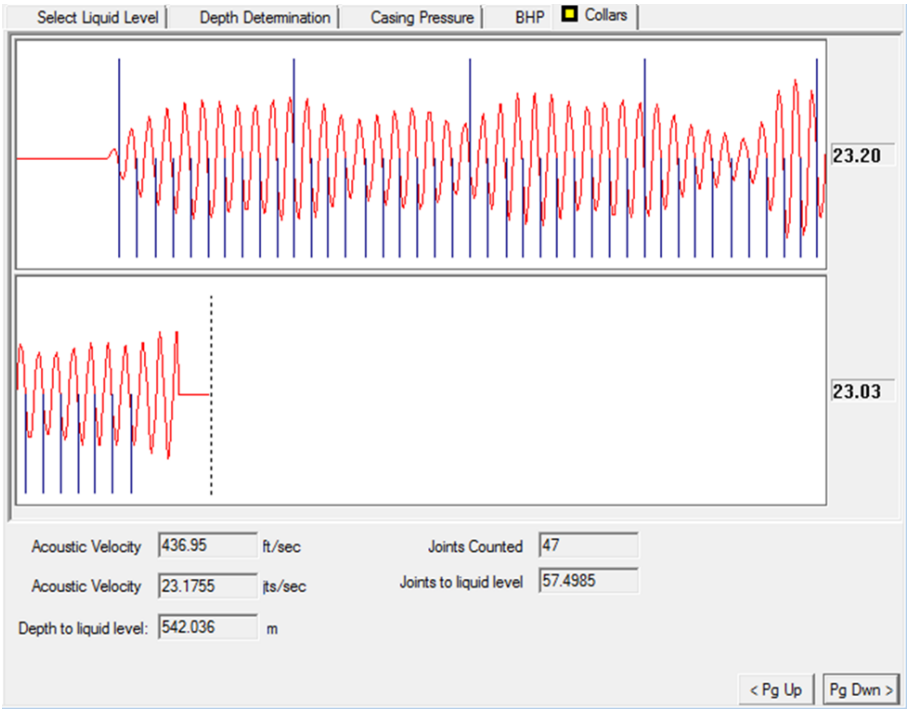

Figure 2.9: An example of collar counting in TWM software

2.6.1.4 Liquid Level Determination Using Downhole Marker

One way to improve the depth and fluid level measurement is to use the depth of known features such as a liner top, tubing anchor, crossovers, or other changes in cross-sectional area as markers to estimate a more representative acoustic velocity. This option is activated by selecting Down Hole Marker as analysis method.

The marker line is adjusted until it matches the signal and known depth to the marker. This yields the acoustic velocity which is then used to compute the fluid level depth from its time.

This method gives an accurate result when liquid level is below the marker such as top of the liner.

2.6.1.5 Liquid Level Determination from Acoustic Velocity

Well defined acoustic records are seldom obtained. The liquid level reflection on acoustic records is often the only interpretable recording. The

distance to the liquid level is determined by integrating the relationship between acoustic velocity and travel time of the reflected wave. The accuracy of this technique depends on the precision of the measured variables; pressure, temperature, gas properties, and the calculated acoustic velocity. The acoustic velocity of a natural gas may be calculated from eqation 2.26. This equation is valid for real gases. The acoustic velocity equation described by equation 2.26 was directed by [21].

$$a = \left[\frac{g_c kRT}{1 - \frac{P}{Z}\left(\frac{\partial p}{\partial Z}\right)_T} \right]^{\frac{1}{2}} \tag{2.26}$$

If all the components are easily evaluated, equation 2.26 is a useful tool to calculate the acoustic velocity of natural gases in the annulus of pumping wells. Gas pressure and temperature are easily measured at the surface and downhole approximations are usually reliable. The expense of evaluating: the heat capacity ration (K), gas compressibility factor (Z), and its partial derivative at constant temperature $\frac{\partial p}{\partial Z}$, for individual pumped wells generally preclude direct measurement. However these properties may be estimated from an equation of state.

Equations of state have been empirically derived for casing head gases by many authors. The eight constant Benedict-Webb-Rubin (BWR) equation of state was used to evaluate PVT behavior and the ration of specific heat for natural gases. The Dranchuck et. al. [8] fit of the BWR equation to the Standing and Katz Z-factor correlations was used to solve gas compressibility factor and its pressure derivatives. The ratio of specific heats was evaluated from the acoustic velocities of internal energy using constants

determined by Hunkinson et. al. [17]. The acoustic velocities of natural gasses may then be calculated as a function of gas gravity, gas pressure, and gas temperature.

The practical use of the above methodology is that the liquid level depth is accurately calculated from information that is easily measured: travel time, gas gravity, casing head pressure, casing head temperature. The depth to the liquid level is obtained by integrating the relationship between acoustic velocity and time. A numerical approximation given by equation 2.27, sums the multiples of time increments and step velocities. A forward looking stepwise procedure is initiated at the wellhead. The measured travel time is divided into sufficiently small time intervals that the acoustic velocity during each time interval is assumed constant. The first step acoustic velocity is calculated from the wellhead pressure and temperature. The step distance is the multiple of the step velocity with the step time interval. The next step pressure and temperature are then calculated and this procedure continues until the liquid level is reached.

$$FL = \sum_{N}^{i=1} a(P,T)_i \Delta t_i \qquad (2.27)$$

2.6.1.6 Limitations

Special precautions must be taken when calculating the liquid level using the time method. The acoustic velocity principle is best applied to wells or gas columns that have a uniform gas composition. Continuous venting of gas at the surface causes the gas composition in the annular space to be uniform. If the gas column has been shut-in for a long period of time, the composition of gas throughout the casing annulus may vary. McCoy [22]

found that acoustic velocity differences of 35% have been noted in individual wells. Variable gas gravity within the casing annulus may preclude meaningful acoustic velocity calculation. The reliability of this calculation is also reduced by the presence of impurities such as hydrogen sulfide, carbon dioxide and inert gases.

Accurate liquid levels are generally obtained during acoustic devices in unobstructed wellbores. Mechanical obstructions blocking the annular passage to the liquid level precludes using acoustic devices. For example, a tubing centralizer located above the liquid level will reflect most of the acoustic energy. In two strings of casing, a liner top may act similarly, obscuring the liquid level. In wells with a foaming annulus, the acoustic wave is absorbed by the foam column preventing the detection of the gas-liquid interface. For these specified cases, the mass balance technique may be applied.

2.6.2 Fully Automated Fluid Level Measurement Tool

Another fluid level measurement tool called MURAG-20 was developed and presented by RAG Company in Austria, 2010. This fully automated electronic tool is mounted on the casing valve with zero emissions on the environment. This system is simple to maintain due to its easy access on surface location.

MURAG-20 has the capability to provide one fluid level measurement per minute. The measured fluid level data can be transmitted via SCADA (Supervisory Control and Data Acquisition) systems. The availability of online fluid level data enables all kinds of pumps (e.g. ESP, Sucker Rod, PCP) to be operated safely at higher production rates [32].

2.6.2.1 Measurement of fluid level by MURAG-20

The fully automated fluid level measurement tool is comprised of two main components, the measurement device, and the evaluation unit as shown in figures 2.10, and 2.11 respectively. These components are connected to each other by cable. The measurement device is mounted on the opened casing valve and couples different types of electronically generated signals in to the casing annulus. Recording of the back transmitted signals from the well is the second function of this component. These signals are transmitted via cable to the evaluation unit. Identification of the fluid level by digital signal processing and storing the measured data are the functions of this unit.

Figure 2.10: MURAG-20 transducer [6]

Figure 2.11: MURAG-20 analyzer [6]

The fluid level is permanently displayed and available via a 4-20 mA interface for SCADA systems [5]. Signal processing and measured fluid level are shown in figure 2.12.

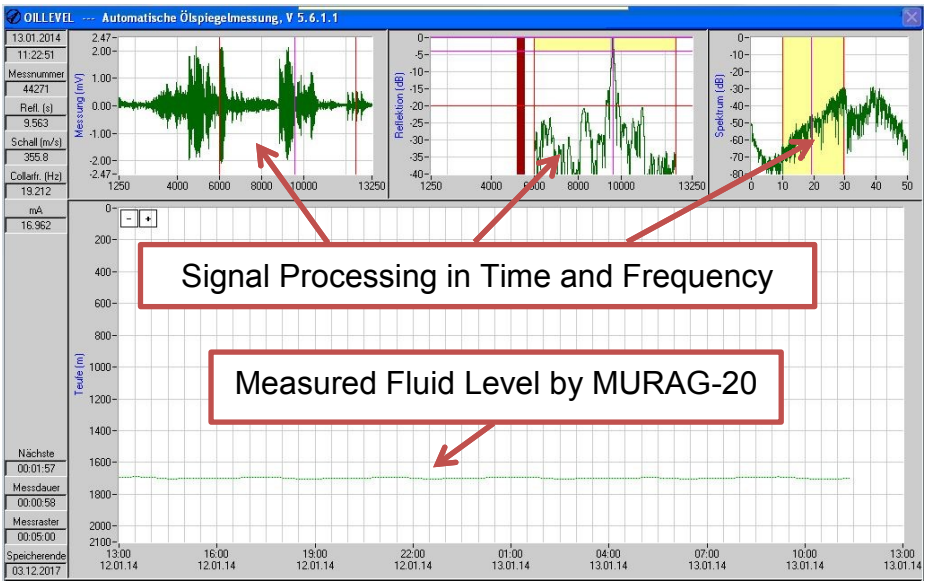

Figure 2.12: Signal processing and measured fluid level from MURAG-20 device

CHAPTER 3: METHODOLOGY AND DATA COLLECTION

An estimation of bottomhole pressure is instrumental in computing a well's performance. One of the most popular methods of estimating bottomhole pressure in pumping wells is the use of fluid level measurement data.

Locating the gas/liquid interface in pumping wells allows the calculation of bottomhole pressure. Bottomhole pressure is the sum of three components: surface pressure, gas column pressure, and liquid column pressure. The surface pressure may be measured directly at the wellhead and should be as accurate as desired. The accuracy of the surface measurement depends on the precision of the pressure instrument.

From the knowledge of the lengths of gas and liquid columns, bottomhole pressure can be estimated by adding the pressures exerted by these columns to the surface pressure (casinghead pressure).

Two deviated pumping oil wells called V-043 and BH-003 owned by RAG Company were selected for bottomhole pressure calculation. Both of those wells have SRP (Sucker Rod Pump) installed. Those wells are completed in a conventional fashion, without a packer. During production, the produced liquids are pumped from the well through the tubing string, while free gas and solution gas travels up the tubing/casing annulus and is produced as casinghead gas at the surface. The MURAG-20 tool has been installed on those wells to determine the depth to the gas/liquid interface. The measurements are taken approximately every five minutes by MURAG-20.

In the following sections, the methods used and assumptions made to calculate bottomhole pressure will be discussed. The methods and

assumptions to calculate bottomhole pressure are the same for both of the studied wells, so they will be explained only one time.

3.1 Numerical calculation of bottomhole pressure using Prosper and Excel software based on fluid level data

A numerical procedure was employed handled with a Prosper-built well model.

In the first step, the well model was built using Prosper software to obtain PVT data of each well. Since liquid and gas properties change with depth, these PVT data were acquired as a function of pressure and temperature and put into a table. Pressure gradients above and under the pump were extracted from Prosper employing the “Petroleum Experts 2” correlation as well. The flow pattern detected by Prosper in the liquid column was bubble flow. The deviation table including measured depths and their associated true vertical depths and dips was constructed for each well.

Both of the wells produce from reservoir at pressures less than the bubble point pressure of the virgin oil liquid, dissolved gas, and free gas coexists in the reservoir and flow into the wellbore.

The fluid distribution in the annulus is a function of the producing conditions of the particular well. The situation found in this study was: the fluid level is above the pump and casinghead gas is produced. This condition results in gaseous annular liquid (oil) column. At stabilized producing conditions, the oil in the annulus becomes saturated with the gas that is continuously flowing to the surface.

Two different situations were taken into account for bottomhole pressure calculation: steady state and transient condition. Operationally, the

steady state in pumping wells is achieved when a constant liquid level is maintained while surface gases and liquids are produced at constant rates. Once both the annular vent and pump have been shut in and the buildup test is initiated, then, the transient condition in pumping wells is introduced. At this condition, the fluid level is not constant any more, and rises up the annulus. Since the pressure increases across the annulus (back pressure increases), fluid influx gets less and less until static equilibrium is reached and liquid level does not change.

The only operational difference between BH-003 and V-043 wells arose at transient condition as the casinghead valve was left open after shutting off the pump for V-043 while it was closed for BH-003 well. However, this difference does not influence the calculation process.

In the next sections the employed method to calculate bottomhole pressure at steady state and transient condition will be described.

3.1.1 Bottomhole pressure calculation at steady state

Using Prosper software made the calculation of bottomhole pressure straight forward as gradient above and under the pump were simply obtained from Prosper.

The gas pressure at the fluid level was calculated using measured casing pressure at surface and the pressure exerted by the gas column on the fluid level, as follows:

$$P_{FL} = P_{CASING} + (FL_{TVD} * g * P_{CASING})/100000 \quad (3.1)$$

As can be seen in equation 3.1, casing pressure was used instead of using gas density for simplicity to calculate pressure exerted by the gas column. The pressure at the fluid level is casing pressure plus weight of the

gas column. This is basically what the equation says, just for the sake of simplicity ideal gas properties were assumed, therefore, gas density = 100000/pressure.

Accurate calculations of gas column pressure increase at steady state with this method required the gas composition to be constant within the annular gas space.

In the next step, the pressure at pump depth was calculated by adding the calculated pressure at fluid level and the amount of pressure exerted by the fluid column above the pump, as follows:

$$P_{PUMP} = P_{FL} + (Pump\ Depth_{TVD} - FL_{TVD}) * PG_{ABOVE\ PUMP} \quad (3.2)$$

Downhole pressure gauge installation in V-043 well makes another difference compared to BH-003 well, as BH-003 has not been equipped with such equipment. The downhole pressure gauge in V-043 well made it possible to compare the measured pressure to the calculated pressure at gauge depth, and evaluate the accuracy of the employed method. Pressure at gauge depth was calculated using equation 3.3 for V-043 well, as follows:

$$P_{GAUGE} = P_{PUMP} + (Gauge\ Depth_{TVD} - Pump\ Depth_{TVD}) * PG_{UNDER\ PUMP} \quad (3.3)$$

Finally, the pressure at perforation was calculated using equation 3.4 as follows:

$$P_{PERF} = P_{PUMP} + (Perforation\ Depth_{TVD} - Pump\ Depth_{TVD}) * PG_{UNDER\ PUMP} \quad (3.4)$$

3.1.2 Bottomhole Pressure Calculation at Transient Condition

In this section, the utilized method to calculate bottomhole pressure at transient condition will be described.

The buildup was initiated by stopping the pump cycle and allowing the wellbore to fill up. Liquid after flow was monitored from the MURAG-20 fluid

level measurements. The surface annulus pressure (casing pressure) and the liquid level movement were recorded as a function of time.

At the first place, the volume of liquid in wellbore was estimated by equation 3.5:

$$Volume\ Of\ Liquid_{WELLBORE} = Volume\ Under\ Pump + 7inch\ Annulus\ Area * (Anchor\ Depth_{MD} - FL_{MD}) \quad (3.5)$$

Where $Volume\ Under\ Pump$ and $7inch\ Annulus\ Area$ were calculated using equations 3.6 and 3.7 respectively.

$$Volume\ Under\ Pump = 7inch\ liner\ Area * (Perforation\ Depth_{MD} - Tubing\ Depth_{MD}) + 7inch\ Annulus\ Area * (Tubing\ Depth_{MD} - Anchor\ Depth_{MD}) \quad (3.6)$$

$$7inch\ Annulus\ Area = \frac{\pi}{4} * (CASING\ ID^2 - TUBING\ OD^2) \quad (3.7)$$

And, 7inch liner area was calculated as follows:

$$7inch\ Liner\ Area = \frac{\pi}{4} * CASING\ ID^2 \quad (3.8)$$

In the next step, the volume of water in wellbore was estimated as follows:

$$Volume\ of\ Water\ in\ Wellbore = [Volume\ Under\ Pump + (FL\ Right\ Before\ ShutIn_{TVD} - Current\ FL_{TVD}) * 7inch\ Annulus\ Area] * WC \quad (3.9)$$

As equation 3.9 shows, the fluid level right before shut in was used to be subtracted by the current fluid level to estimate the volume of liquid entering the wellbore at each specific fluid level measurement.

Then, the volume of oil in wellbore was simply estimated using equation 3.10.

$$Volume\ of\ Oil\ in\ Wellbore = Liquid\ in\ Wellbore - Water\ in\ Wellbore \quad (3.10)$$

Since there is only liquid below the pump, by having the volume of oil in wellbore and estimating the volume of liquid in annulus, comparison of these two volumes made it possible to identify if the oil column was only limited to above the pump and along the annulus or it was present below the pump as well. For this reason, the volume of liquid in annulus was calculated using equation 3.11.

$$Volume\ of\ Liquid\ in\ Annulus = (Tubing\ Depth_{MD} - FL_{MD}) * 7inch\ Annulus\ Area \quad (3.11)$$

At this step, the length of the oil column corresponding to each fluid level measurement could be estimated at two different conditions; the first condition was when the volume of oil in wellbore was bigger than the volume of the liquid in annulus, and the oil column had been stretched to below the pump, despite to above it. And the second condition was when the oil volume in wellbore was less than the volume of liquid in annulus and the oil column was only restricted to the space above the pump and annulus. Equations 3.12 and 3.13 are employed to calculate the length of the oil column at former and latter conditions respectively.

$$Length\ of\ Oil\ Column = (Tubing\ Depth_{MD} - FL_{MD}) + (Volume\ of\ Oil\ in\ Wellbore - Volume\ of\ Liquid\ in\ Annulus) / 7inch\ Liner\ Area \quad (3.12)$$

$$Length\ of\ Oil\ Column = Volume\ of\ Oil\ in\ Wellbore / 7inch\ Annulus\ Area \quad (3.13)$$

The accuracy of calculating pressure increase in the oil column depends on how well known are the fluid state and physical processes in the wellbore. The calculation is straight forward when dead oil columns are considered. Uncertainty arises in the oil column when gas is present, vented through or in solution in the liquid column (oil column). The flow of gas

through oil columns has a profound effect on the annulus oil pressure gradient.

To determine the pressure change in the gaseous oil column, an estimation of the gas void fraction (f_g) in the oil column is required. A correlation presented by Hasan and Kabir [20] (equation 3.18) that relates superficial gas velocity (v_{sg}) to the gas void fraction was employed.

As the pressure increases, the amount of oil and gas entering the wellbore decreases. Therefore, gas flowing into the annular gas space from the liquid column decreases as less gas enters the wellbore and less solution gas is liberated from the oil column as a result of pressure increase.

To determine the superficial gas velocity, a reasonable estimate of the fluid entering the wellbore was obtained by employing the concept of Inflow Performance Relationship (IPR). To do so, at first, straight line IPR which is not applicable for multiphase flow was used only to calculate Productivity Index (PI) of the well (equation 3.14). Then, putting wellbore flowing pressure (P_{wf}) in the PI's formula to zero, q_{MAX} was acquired (equation 3.15). Then, Fetkovitch method [12] was applied to estimate the sand face flow rate at each fluid level measurement (equation 3.16). Eventually, superficial gas velocity (equation 3.17) and finally gas void fraction (equation 3.18) were calculated using a new flow rate at each measurement.

$$PI = \frac{q}{P_r - P_{wf}} \tag{3.14}$$

$$q_{MAX} = PI * P_r \tag{3.15}$$

$$q = q_{MAX} * [1 - (\frac{P_{wf}}{P_f})^2] \tag{3.16}$$

$$v_{sg} = \frac{q_{MAX} * [1 - (\frac{P_{wf}}{P_r})^2] * GOR * B_g}{Flow\ Area} \quad (3.17)$$

$$f_g = \frac{v_{sg}}{(1.97 + 0.371 * \frac{TUBING\ OD}{CASING\ OD}) * (v_{sg} + v_{sl})} + \frac{v_{sg}}{1.5 * [g * \sigma * \frac{(\rho_o - \rho_g)}{\rho_o^2}]^{0.25}} \quad (3.18)$$

In equation 3.17, Gas/Oil Ratio (GOR) was a constant value throughout the calculation and Gas Formation Volume Factor (B_g) was obtained using a lookup function in Excel from a Prosper acquired PVT table for each depth and corresponding pressure and temperature.

In equation 3.18 to calculate gas void fraction, superficial liquid velocity (v_{sl}) was neglected due to being very low compared to the superficial gas velocity.

Oil density (ρ_o) and gas density (ρ_g) were extracted from PVT table for each measurement.

Interfacial tension between oil and gas (σ) were the same and equal to 40 $(\frac{dyne}{cm})$ for both of the wells.

The basic uncertainty in calculating bottomhole pressure in pumping wells arises within a gaseous liquid column when free gas bubbles through. The process of gas bubbling through a static liquid column may have an important effect on the pressure gradient.

The process of gas bubbling through an oil column is complex to model. Fluids entering the wellbore segregate by density, free gas migrates upward leaving the heavier components behind. Equilibrium oil and dissolved gas results, with free gas travelling through. The equilibrium column is

simplified by considering a dead oil column, and then investigating the effects of dissolved gas. Free gas is superposed in the oil column to complete the pressure calculation.

Podio et al. [27] determined that the superficial gas velocity was an improved correlating parameter for gaseous liquid columns. The S-Curve presented by Podio et. al. [27] (Figure 3.1) is an example of applying the concept of adjusted fluid level depth (D_a) to correct the calculation of bottomhole pressure for gas fraction in gaseous liquid columns. It was carried out at standard conditions of pressures and temperatures, $14.7\ psig\ [101.3KPa]$ and $60^o F\ [15.5^o C]$.

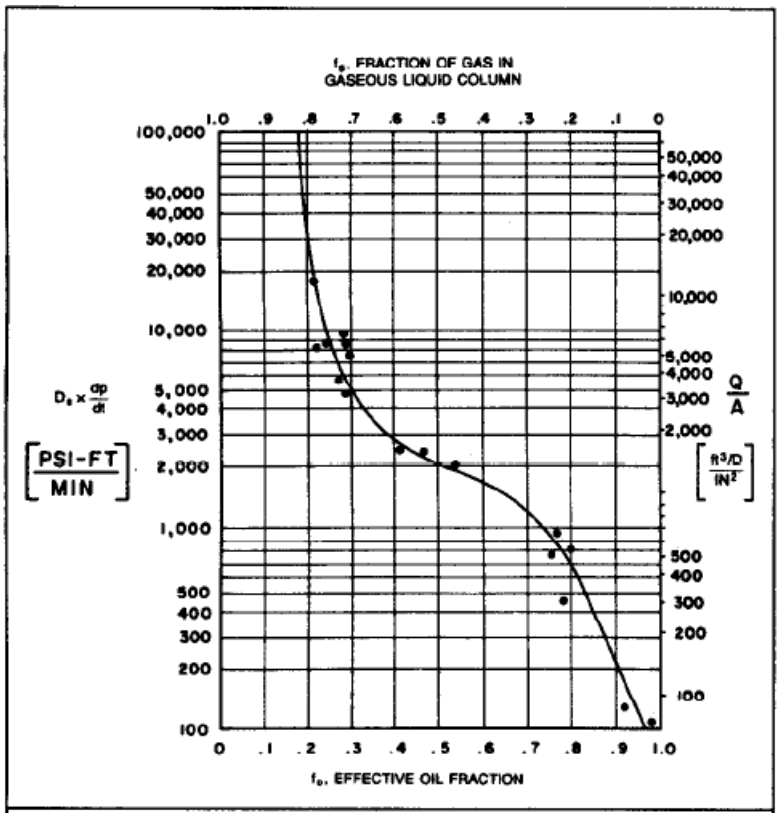

Figure 3.1: Gaseous liquid column gradient correction curve (S-Curve) [27]

At this point, the concept of adjusted fluid level depth was applied in the method employing equation 3.19, where the gas fraction was obtained from equation 3.18.

$$D_{a_{MD}} = FL_{MD} + (f_g * Oil\ Column\ Length) \tag{3.19}$$

Using the concept of adjusted fluid level depth, the originally gaseous oil column was divided into a pure gas column and a dead oil column enabling the use of a dead oil pressure gradient in the oil column. To calculate bottomhole pressure, true vertical depth of adjusted fluid level was needed. So, true vertical depth of $D_{a_{MD}}$ was calculated for each fluid level measurement.

New Pressure at fluid level was then calculated using D_a which was called “New Pressure at Fluid Level” to differentiate it from “Pressure at Fluid level” calculated at steady state.

$$New\ P_{FL} = P_{CASING} + (D_a * g * P_{CASING})/100000 \tag{3.20}$$

The measure depth of water top using equation 3.21 was estimated.

$$Water\ Top\ Depth_{MD} = D_a + (1 - f_g) * Oil\ Column\ Length \tag{3.21}$$

Equation 3.21 was employed to convert the estimated measured depth of water top to true vertical depth. In equation 3.22, deviation table was used applying a lookup function in Excel for each measured fluid level based on estimated measured depth of water top.

$$\begin{aligned} Water\ Top\ Depth_{TVD} &= (TVD\ Based\ on\ Water\ Top\ Depth_{MD}) + \\ &(Water\ Top\ Depth_{MD} - MD\ Based\ on\ Water\ Top\ Depth_{MD}) * \\ &COS(DIP\ Based\ on\ Water\ Top\ Depth_{MD} * \frac{\pi}{180}) \end{aligned} \tag{3.22}$$

The next step was dedicated to pressure estimation exerted by dead oil column after separating from gas column using adjusted fluid level depth

concept. To do so, an average oil gradient across the oil column was evaluated. An oil gradient called $Oil\ Gradient_1$ was obtained at the fluid level for each measured fluid level using a lookup function from PVT table already put in to an Excel sheet based on its associated $New\ P_{FL}$. The estimated $Oil\ Gradient_1$ was employed to obtain pressure estimate at water top using equation 3.23 as follows:

$$P\ Estimate\ at\ Water\ Top\ Depth_{TVD} = New\ P_{FL} + (Water\ Top\ Depth_{TVD} - D_{a_{TVD}}) * Oil\ Gradient_{\ 1} \quad (3.23)$$

After obtaining $P\ Estimate\ at\ Water\ Top\ Depth_{TVD}$, $Oil\ Gradient_2$ was estimated similar to the $Oil\ Gradient_1$ but based on associated $P\ Estimate\ at\ Water\ Top\ Depth_{TVD}$ for each measured fluid level.

$Mean\ Oil\ Gradient$ was then estimated by averaging $Oil\ Gradient_1$ and $Oil\ Gradient_2$, as follows:

$$Mean\ Oil\ Gradient = \frac{Oil\ Gradient_1 + Oil\ Gradient_2}{2} \quad (3.24)$$

As it was mentioned, the main difference between V-043 and BH-003 wells is that V-043 well is equipped with downhole pressure gauge, but BH-003 is not equipped with it. So, P_{GAUGE} was estimated for V-043 well considering a condition, if the calculated $Water\ Top\ Depth_{MD}$ was above or below the gauge depth.

Equation 3.24 was used to estimate P_{GAUGE}, if $Water\ Top\ Depth_{MD}$ was deeper than the gauge depth.

$$P_{GAUGE} = New\ P_{FL} + (Gauge\ Depth_{TVD} - D_{a_{TVD}}) * Mean\ Oil\ Gradient \quad (3.25)$$

To calculate P_{GAUGE} when $Water\ Top\ Depth_{MD}$ was located above the gauge depth, $P_{WATER\ TOP}$ and $Mean\ Water\ Gradient$ across the water column were required to be estimated. Equation 3.26 was used to evaluate pressure at water top.

$$P_{WATER\ TOP} = New\ P_{FL} + (Water\ Top\ Depth_{TVD} - D_{a_{TVD}}) * Mean\ Oil\ Gradient \quad (3.26)$$

To estimate $Mean\ Water\ Gradient$ the same procedure as utilized to estimate $Mean\ Oil\ Gradient$ was used. First, $Water\ Gradient_1$ was obtained from PVT table using a lookup function based on calculated $P_{WATER\ TOP}$ for each measured fluid level. Then, a $P\ Estimate\ at\ Perforation$ was calculated using equation 3.27. In the next step, $Water\ Gradient_2$ was acquired utilizing a lookup function based on $P\ Estimate\ at\ Perforation$ for each fluid level measurement. Calculating $Mean\ Water\ Gradient$ by equation 3.28, P_{GAUGE} was calculated applying equation 3.29.

$$P\ Estimate\ at\ Perforation = P_{WATER\ TOP} + (Perforation\ Depth_{TVD} - Water\ Top_{TVD}) * Water\ Gradient_1 \quad (3.27)$$

$$Mean\ Water\ Gradient = \frac{Water\ Gradient_1 + Water\ Gradient_2}{2} \quad (3.28)$$

$$P_{GAUGE} = P_{WATERTOP} + (Gauge\ Depth_{TVD} - Water\ Top\ Depth_{TVD}) * Mean\ Water\ Gradient \quad (3.29)$$

Finally, P_{PERF} was calculated applying the equation 3.29 at transient condition.

$$P_{PERF} = P_{Water\ Top} + (Perforation\ Depth_{TVD} - Water\ Top_{TVD}) * Mean\ Water\ Gradient \quad (3.30)$$

The procedures to calculate bottomhole pressure at both steady state and transient condition are shown in appendix B-1 and B-2.

3.2 Numerical calculation of bottomhole pressure using Prosper and VB-Script based on fluid level data

This method was applied only on V-043 well to calculate bottomhole pressure at steady state and transient condition based on fluid level data.

First of all, the well model was built using Prosper software similar to the previous method and the measured fluid levels versus time along with

their associated casing pressures where inserted into an Excel sheet. Constant values of oil flow rate (q_o), water flow rate (q_w), and gas/oil ratio (GOR) at steady state and fixed values of measured and two vertical depths of perforation and gauge depth put into another sheet of Excel.

As Prosper is a steady state tool and it does not model transient phenomena, and as PVT correlations work only for steady state, this method was proposed to apply Prosper as a transient tool.

To do so, visual basic programming in Excel was done, then the codes were linked to Prosper via OpenServer.

OpenServer is a powerful utility that allows other programs (such as Excel, Programs written in Visual Basic) to access public functions in IPM (Integrated Production Modeling) toolkit generated by PETEX (Petroleum Experts) to automate data input and model calculations. Specifically, OpenServer allows other programs such as Excel, or programs written in Visual Basic, to access public functions in the IPM suite of tools. OpenServer can be used to run the IPM suite of tools in conjunction with other software applications and exchange data between them [26].

The proposed method is to divide the well into ten-meter segments and calculate the pressure gradient across each segment. Summing up the pressure gradients of all segments along the wellbore yields the pressure at perforation. Doing so, it can be assumed that the well as a whole is not at steady state, while each segment can be assumed to be at steady state.

To calculate the bottomhole pressure using fluid level data, a datum pressure is needed as the starting point. Since casing pressures associated

with each measured fluid level were known, they were used as the datum pressures.

In the first step, it was programmed to divide the well from the wellhead to the perforation considering ten-meter depth intervals. All calculations were done for one interval and after adding the interval by ten meters and shifting to the next interval, the same calculations were carried out for the new interval, continuing this procedure until the perforation depth was reached.

The next step was dedicated to determining true vertical depth, casing ID, tubing OD and cell volume corresponding to each individual interval. It was carried out by comparing each measured depth (individual intervals) with the deviation survey and downhole equipment sub-sections in equipment data section of the built Prosper model after connecting VB-Script to Prosper model via OpenServer.

Cell volume was calculated as follows:

$$Cell\ Volume = (CASING\ ID^2 - TUBING\ OD^2) * \frac{\pi}{4} * Interval \tag{3.31}$$

To calculate the bottomhole pressure using fluid level data, the starting point was the casinghead pressure. For each interval, the downstream values (closer to the wellhead) of pressure were known. These values were put into Prosper software as first node pressures for associated intervals. Bottomhole pressure was calculated employing this method using fluid level data at two different conditions: when the well was producing at a nearly constant flow rate (steady state condition), and when the pump was shut off and build-up test began which led to transient condition. In the following sections, bottomhole pressure calculation at steady state and transient condition will be detailed.

3.2.1 Bottomhole pressure calculation at steady state

From the casinghead to the fluid level, there is only gas along the annulus. So, the “fluid type” was selected as “dry and wet gas” in Prosper. The “method” was selected as “black oil”, and as the pressure was to be calculated in the annulus, the “flow type” was selected as “tubing + annular flow”. “Condensate/gas ratio” set to zero in Prosper, otherwise the calculated gas density within each interval would be too high. The “gas rate” was set to 1 [m^3/d], because the flow rates only affect the friction term, therefore, as the annulus cross-section is large and the resultant superficial velocities are low, the friction term can be ignored.

To consider the influence of temperature on bottomhole pressure calculation, the “calculation type” in Prosper was selected as “pressure and temperature (on land)”. “Pertoleum Experts 2” correlation was used for pressure calculations.

When upstream values of pressure were calculated, the algorithm advanced to the next wellbore segment and this process was continued until the fluid level was reached.

The same procedure was applied to estimate the pressure within the intervals across the gaseous liquid column and liquid column. First of all, it was programed to change the “fluid type” in Prosper to “oil and water”.

As no liquid would be produced from the annulus, “liquid rate” was set to 1 [m^3/d], as it is not possible to set the value to zero in Prosper for pressure gradient calculations.

“GOR” was set to the constant value which had already been inserted in one of the Excel sheets.

To input “water cut” in Prosper at steady state, two conditions were defined regarding the depth of the considered well interval. It was programmed to set “ water cut” to zero when the depth interval being calculated would be above the pump depth, due to having no water in the annulus above the pump depth at steady state (for oil water separation reasons). When the depth interval was below the pump, “water cut” was calculated using equation 3.32 and put into Prosper.

$$WC = \frac{q_w}{q_w + q_o} \tag{3.32}$$

Finally, using “Petroleum Experts 2” correlation, the pressure gradient within each interval was calculated.

As V-043 well had been equipped with a downhole pressure gauge, first the pressure at gauge depth and then the pressure at perforation were calculated by the summation of the pressure gradients across individual intervals by Prosper.

3.2.2 Bottomhole pressure calculation at transient condition

The principles of the procedure to calculate pressure at gauge and perforation depths is similar to the steady state. The main differences arose from two sources, firstly, changing the employed correlation from “Petroleum Experts 2” to “Duns & Ros Original”, and secondly, estimating “water cut” using equation 3.32 for intervals after selecting “oil and water” as “fluid type”, as the water top depths was always above the gauge depths after pump shut off and moving fluid level upwards.

Applying above changes, the pressures at gauge and perforation depths were finally calculated.

The procedures of calculating pressure at gauge and perforation depths at steady state and transient condition are shown in appendix C-1 and C-2.

CHAPTER 4: RESULTS AND DISCUSSION

As it has been described in the previous chapter, two numerical methods were used to calculate bottomhole pressure.

The first method to calculate bottomhole pressure was using Excel in combination with Prosper. In that method the concepts of adjusted fluid level depth and productivity index coupled with some more correlations,

assumptions, and definitions especially within the gaseous liquid (oil) column were utilized for pressure calculation.

The second method employed Visual Basic programming in Excel along with Prosper software to calculate bottomhole pressure. The Visual Basic script (codes) was connected to Prosper via OpenServer.

The above methods were applied in two deviated oil wells, V-043 and BH-003. In V-043 well, the installed downhole pressure gauge gave the opportunity to compare pressure measured by the gauge to calculated pressure at gauge depth and for checking out the accuracy of the employed method.

This chapter discusses the results obtained from pressure calculations using the two methods and their interpretations. Measured fluid level at steady state and transient condition along the annulus is plotted versus time for each well, and then the effect of fluid level changes on calculated pressures will be described.

4.1 V-043 Well

In this section the results obtained from applying two methods for V-043 well are presented and discussed.

4.1.1 Calculation of bottomhole pressure using Excel and Prosper software based on fluid level data

To check out the accuracy of the method, first of all, the pressures at gauge depth were calculated (using measured fluid levels from MURAG-20 as input data) and compared with the measured pressures from the downhole gauge. Figure 4.1 compares the calculated pressures utilizing this method and the measured pressures.

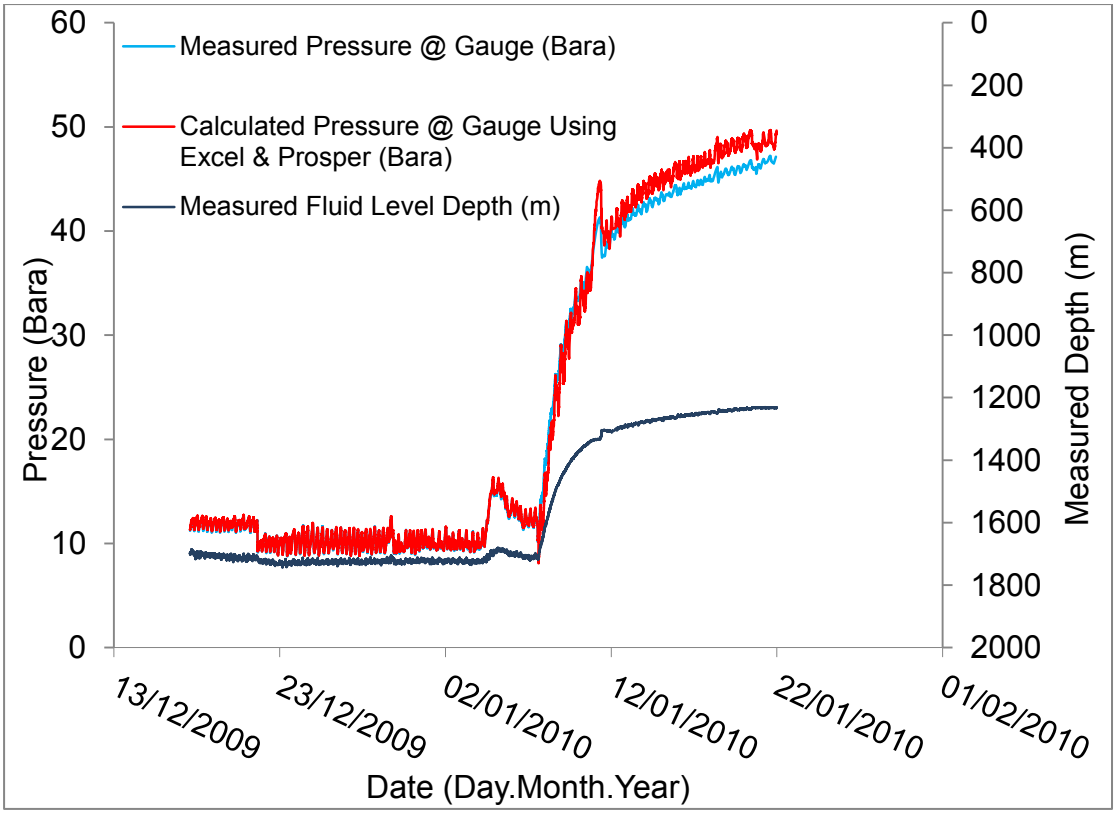

Figure 4.1: Comparison of measured and calculated pressures at gauge using Prosper and Excel software based on fluid level data for V-043 well

As can be seen in figure 4.1, the calculated pressures at steady state are in very good agreement with the measured pressures from the gauge. Once the well is shut in and the build-up test is started (transient condition), the pressure increases. Figure 4.1 indicates that there is a close agreement between the calculated and measured pressures. The difference increases with oil column length. As the amount of solution gas increases and less gas is liberated from oil, this difference increases. Another reason for this difference is due to using “Petroleum Experts 2” correlation in Prosper that is only valid for steady state; while it was used at transient condition also to generate the PVT table.

The effect of fluid level changes on calculated pressures is presented in figure 4.2. As can be observed, there is a direct relationship between the

pressure changes and the fluid level changes (rises). As the fluid level rises, the pressure increases.

Finally, pressures calculated at perforation depth at various measured fluid levels are shown in figure 4.3.

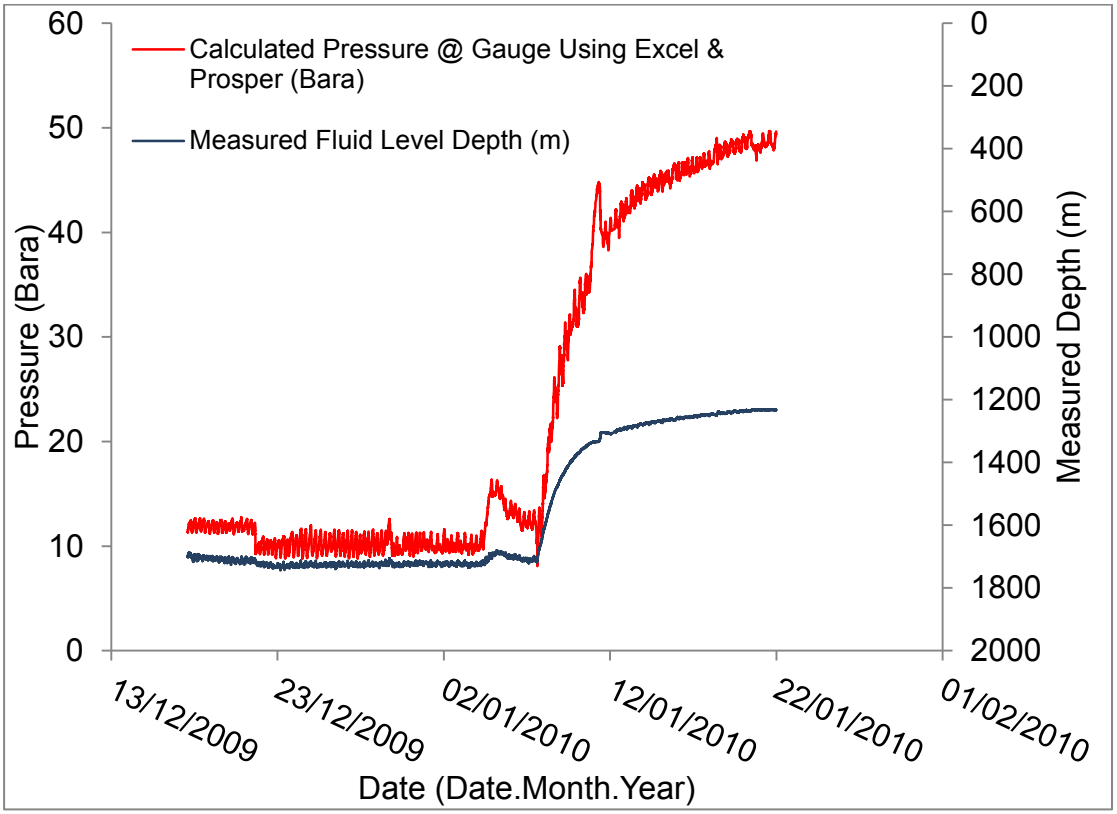

Figure 4.2: The effect of fluid level changes on calculated pressures using Prosper and Excel software based on fluid level data for V-043 well

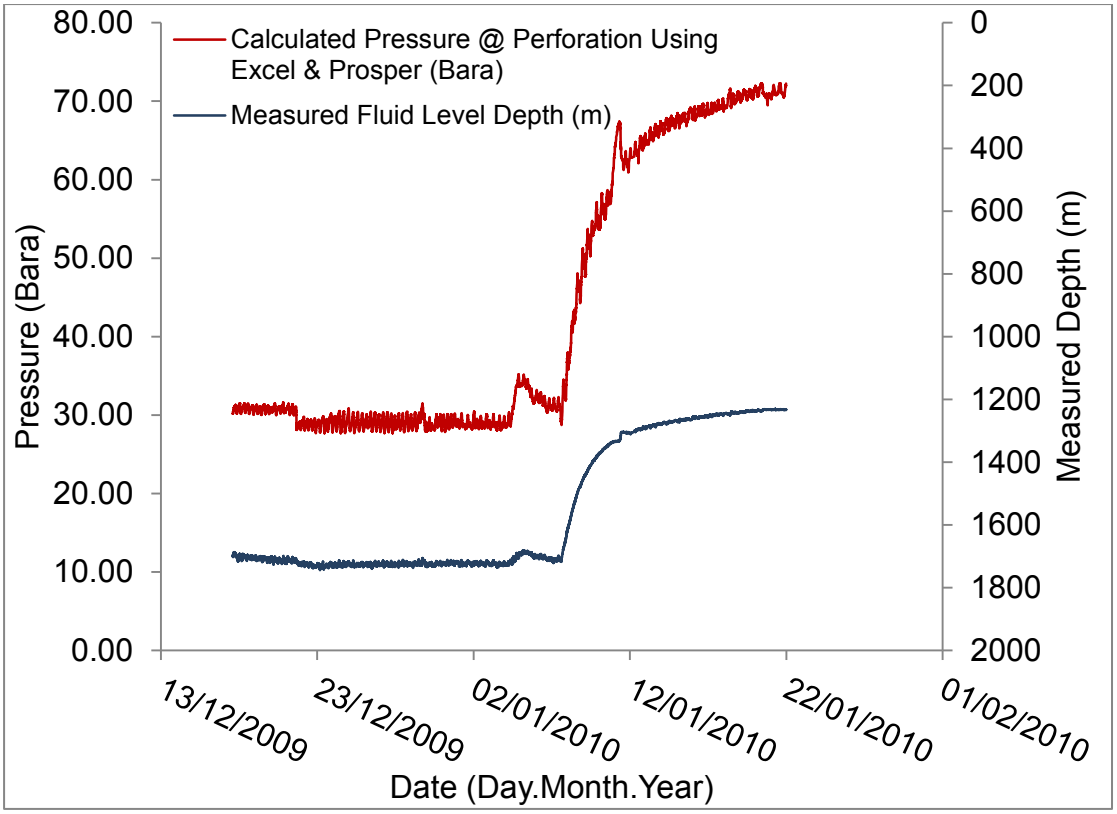

Figure 4.3: Calculated pressures at perforation using Prosper and Excel software based on fluid level data for V-043 well

4.1.2 Calculation of bottomhole pressure using VB-Script and Prosper software based on fluid level data

The pressures calculated at gauge depth are shown in figure 4.4 using Visual Basic programming and Prosper. The comparison of calculated and measured pressures shows a very interesting agreement especially at transient condition. However, the calculated pressures at steady state using this method are close to the measured ones but not as accurate as for transient condition.

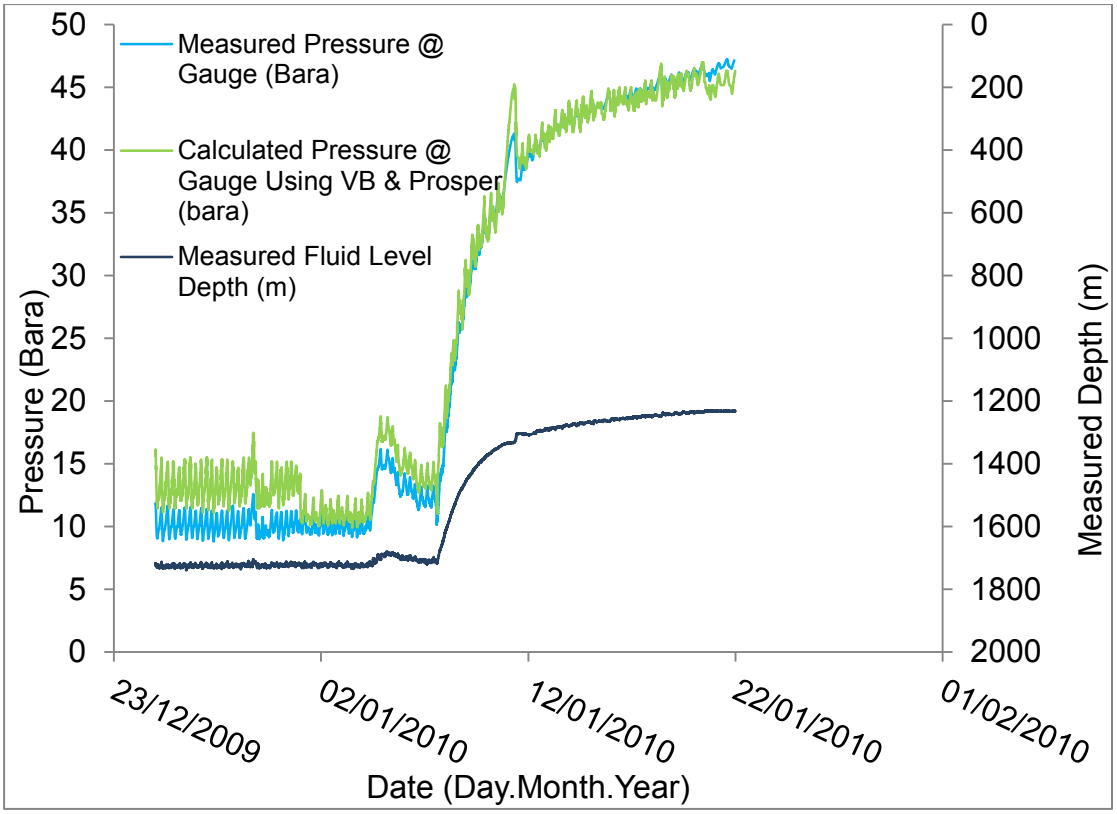

Figure 4.4: Comparison of calculated and measured pressures at gauge using VB-Script and Prosper software based on fluid level data for V-043 well

The calculated pressures at perforation depth employing this method are shown in figure 4.5.

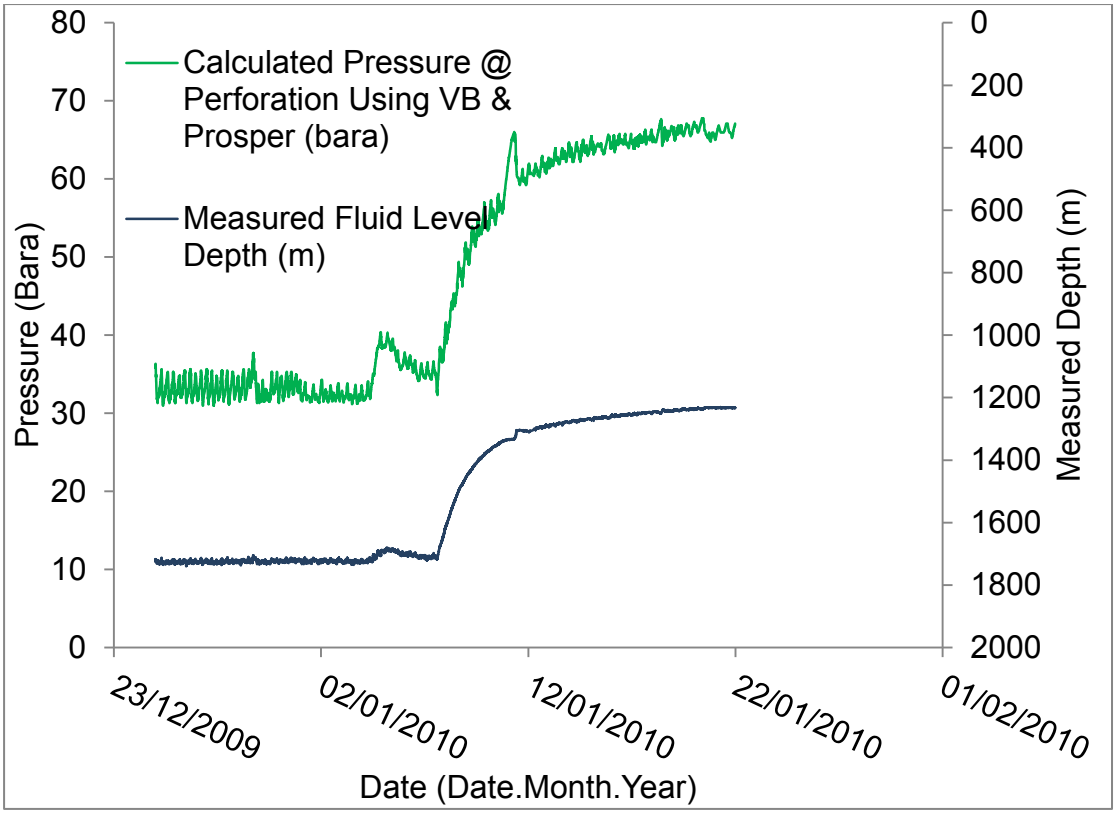

Figure 4.5: Calculated pressures at perforation using VB-Script and Prosper software based on fluid level data for V-043 well

4.1.3 Comparison of calculated pressures at gauge using two methods

The pressures calculated using the two methods are compared with the measured pressures from the downhole gauge as shown in figure 4.6. Both methods present very good results and close agreement with the measured values at transient condition. But at steady state, applying the first method gives better results as can be observed in figure 4.6.

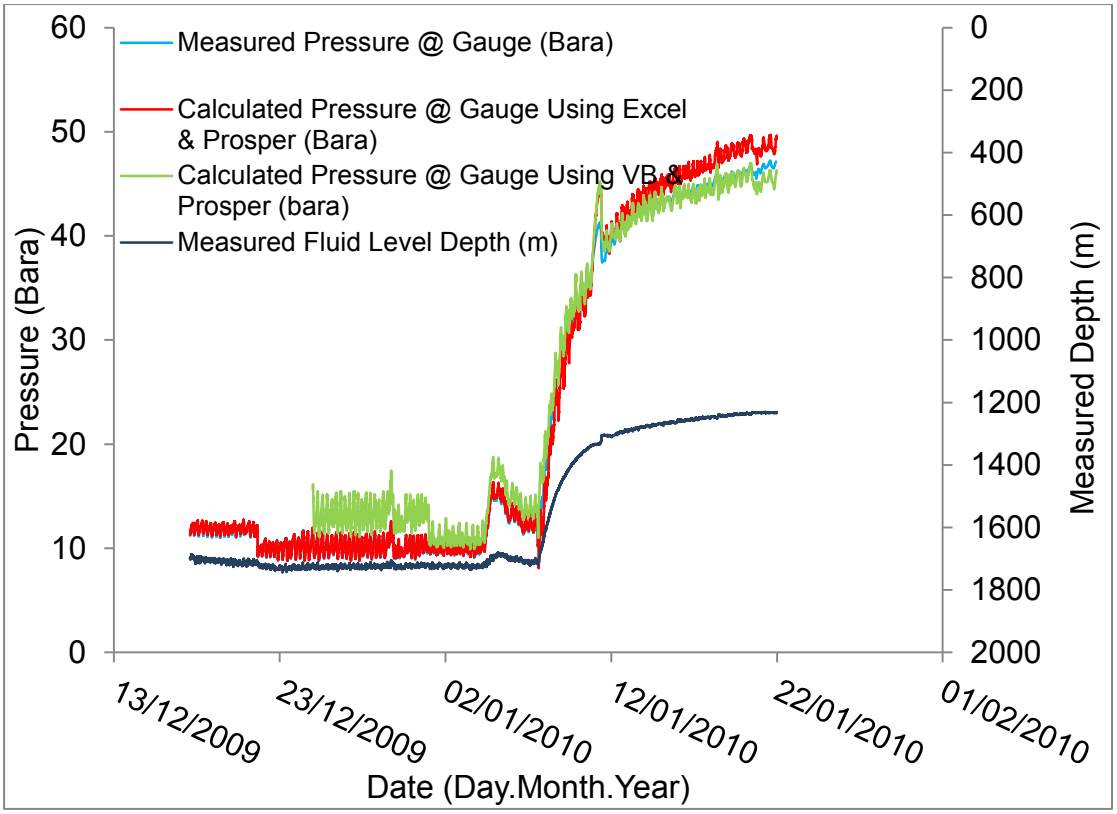

Figure 4.6: Comparison of calculated pressures at gauge using two methods for V-043 well

4.1.4 Comparison of calculated pressures at perforation using two methods

Calculation of pressure at perforation depth is the final objective of utilizing those two methods. Both methods present reliable results at steady state and transient condition. Figure 4.7 indicates the pressures calculated at perforation before and after shutting in the well.

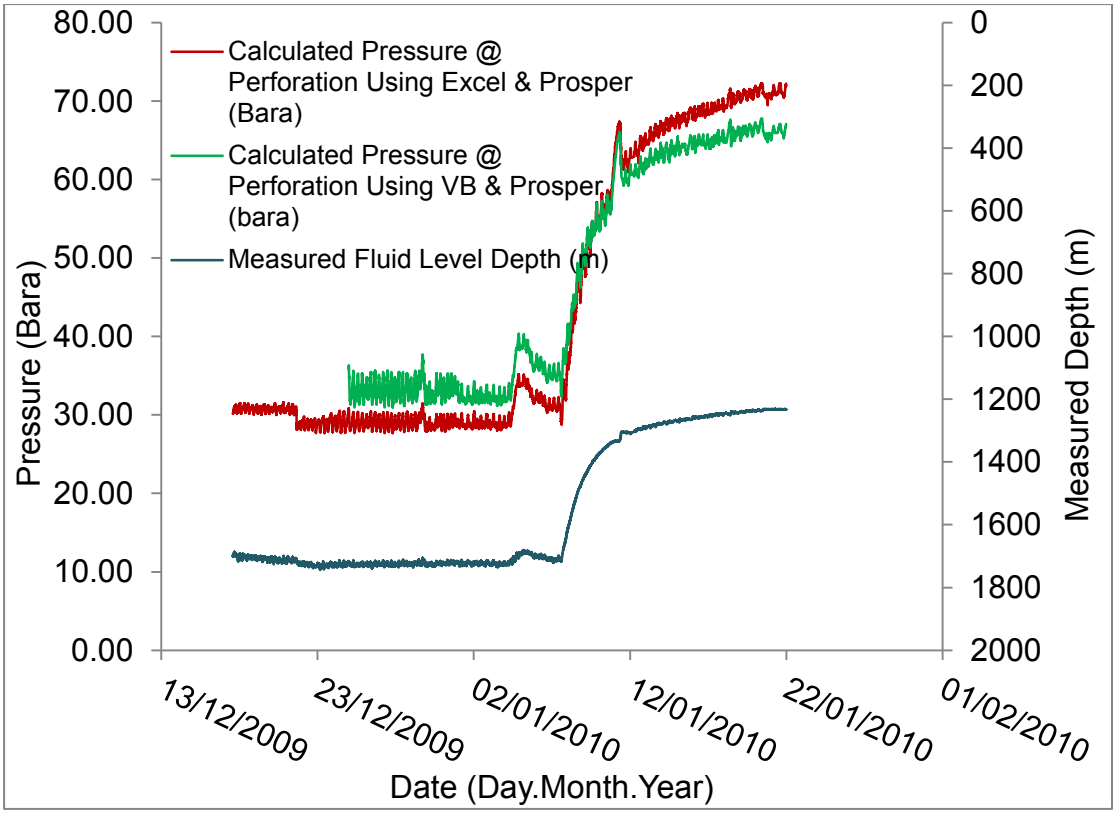

Figure 4.7: Comparison of calculated pressures at perforation using two methods for V-043 well

4.2 BH-003 Well

In this section the results obtained from applying VB-Script and Prosper software method for BH-003 well are presented and discussed.

4.2.1 Calculation of bottomhole pressure using Excel and Prosper software based on fluid level data

As it was already mentioned, BH-003 well has not been equipped with a downhole pressure gauge, so, pressures at different fluid levels were calculated only at perforation depth.

The pressures calculated at perforation using this method are shown versus the dates corresponding to each fluid level measurement in figure 4.8. As can be seen in figure 4.8, the pressure increases as the fluid level rises.

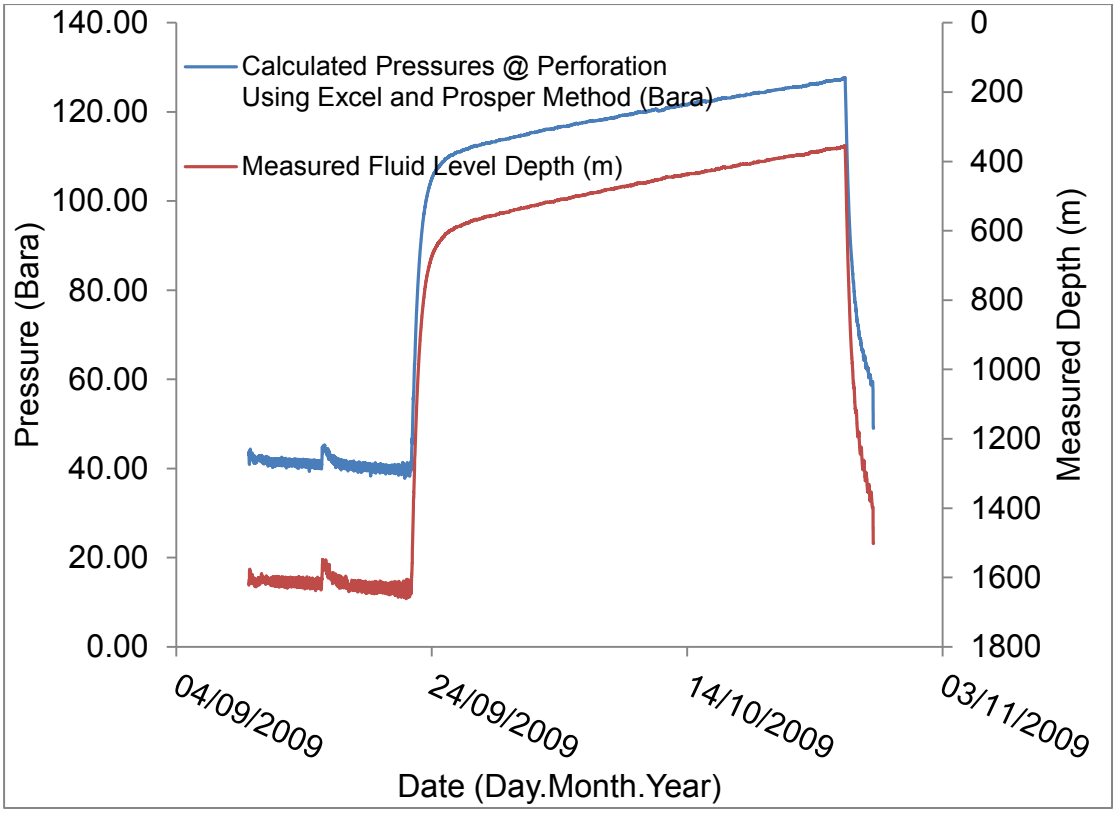

Figure 4.8: Calculated pressure at perforation using Excel and Prosper software based on fluid level data For BH-003 Well

Figure 4.8 shows that after shutting in the well, the rate of pressure build-up is approximately constant up to a point where the rate of pressure increase decreases and gets nearly smooth. This build-up rate continues until the pump is turned on again, and the fluid level and eventually the pressure drop.

Well test interpretation was done using Saphir software package by the reservoir engineering department of RAG Company on the results of Excel and Prosper method for BH-003 well which the extrapolated pressure was very close to the expected reservoir pressure.

CHAPTER 5: SUMMARY, CONCLUSIONS AND RECOMMENDATIONS

This chapter presents the summary and the conclusions of this research and gives recommendations for further extensions of this work.

5.1 Summary

This study demonstrated how the bottomhole pressure at steady state and transient condition can be calculated and interpreted from fluid level measurements taken with the fully automated MURAG-20 device in two pumping oil wells called V-043 and BH-003.

Two different approaches for steady state and transient condition multiphase flow to calculate bottomhole pressure were presented in detail.

The first method was used to overcome the complexity of the bottomhole pressure calculation in multiphase flow using fluid level measurement data after well shut-in and starting pressure build-up utilizing the concept of adjusted fluid level depth with some modifications and improvements.

The second method was applied only on V-043 well to calculate bottomhole pressure using Visual Basic programming in Excel and connecting the written codes to Prosper software via OpenServer. The proposed approach was dividing the wellbore into 10-meter intervals and calculating pressure within each individual interval.

Fluid properties were calculated using BlackOil model for both methods in Prosper.

At the end, the accuracy of the methods were investigated by comparing the calculated pressures with measured pressures from a

downhole pressure gauge (for V-043 well) and well test interpretation results (for BH-003 well).

5.2 Conclusion

A fairly good agreement with the field data was achieved employing the first described method in chapter 3 (Excel coupled with Prosper) for V-043 well at steady state and transient condition (about 1.5% deviation from the real values).

The obtained results from the first method for BH-003 well also indicated a very good accuracy (about 1.5% deviation from the real values) after well test interpretation using the Saphir software package by the reservoir engineering department of RAG Company.

The accuracy of the first method reduces as the length of the oil column increases. This happens due to less and less gas liberation from the oil column as the pressure increases along the wellbore annulus after pump shut-off.

The simplicity of this method to be implemented on other oil wells is one of the noted advantages of it. Considering different physical phenomena at steady state and transient condition should be mentioned as another advantage of this method.

The second method (VB-Script along with Prosper) which was only applied on V-043 well presented a very close agreement with the real data (less than 0.5% deviation from the real values). The accuracy of this method especially during build-up test is excellent and promising.

The second method is highly dependent on the selected pressure gradient correlation in Prosper for pressure calculation, and pressure

correlation matching should be carried out with the measured field data to check out the accuracy of the method.

Both of the methods could be utilized instead of installing a downhole pressure gauge in the well to calculate pressure at each specific depth. As the result, using these methods is very cost effective.

Using these methods, it is avoided to retrieve downhole equipment such as rod, downhole pressure gauge, and etc. Therefore, the great amount of cost and time could be saved.

The VB-Prosper method gave a good match with the field data; nevertheless, it is time consuming for the simulation to be run.

Prosper on its own is not capable of calculating pressure at transient condition and has to be combined with another software for this purpose.

5.3 Recommendations

The presented methods were applied only on two wells, so, it is recommended to employ them on more wells.

There are other software packages such as OLGA for multiphase flow modelling which could be used to check out the accuracy of the methods.

As the methods have been developed only for oil wells, it is recommended for further works to modify them for gas wells as well.

REFRENCES

[1] Beggs, H. D. and Brill, J. P.: “A Study of Two-Phase Flow in Inclined Pipes,” Journal of Petroleum Technology, May 1973, 607-617.

[2] Brennen, C.E. 2005. “Fundamentals of Multiphase Flow.” Cambridge University press. ISBN 0-521-84804-0.

[3] Brill, J.P. 1987. “Multiphase Flow in Wells.” J Pet Technol: 15-21. Distinguished Author Series. SPE 16242-PA.

[4] Brill, J.P. and Mukherjee, H. 1999. “Multiphase Flow in Wells.” Monograph series, SPE, Richardson, Texas 17: 2-69.

[5] Burgstaller, Christian. "Fully Automated Fluid Level Measurement Tool." Gas Well Deliquification Workshop. RAG Company. 17-20 Feb 2013. Speech.

[6] Chaudhry, Amanat U. “Oil Well Testing Handbook.” USA : Elsevier Inc., 2004.

[7] Chen, Y.: “Modeling Gas- Liquid Flow in Pipes: Flow Pattern and Transitions and Drift-Flux Modeling,” Master of Science Report, Stanford University, 2001.

[8] Dranchuk, P. M., R. A. and Robinson, D. B. : “Computer Calculations of Natural Gas Compressibility Factors Using Standing and Katz Correlations,” Inst. Of Petroleum Technical Series, No. IP 74-008, 1974

[9] Duns, H. Jr. and Ros, N. C. J.: “Vertical Flow of Gas and Liquid Mixtures in Wells,” Proceeding of the Sixth World Petroleum Congress, Frankfurt, June 1963, Section II, Paper 22-PD6.

[10] Ellul, I.R., Saether, G. and Shippen, M.E. 2004. “The Modeling of Multiphase Systems under Steady-State and Transient Conditions” – A

Tutorial. PSIG 0403 presented at the PSIG Annual Meeting, Palm Springs, California, 20-22 October.

[11] Fancher, JR.G.H and Brown, K.E. 1963. “Prediction of Pressure Gradients for Multiphase Flow in Tubing.” SPE J: 59-69. SPE 440-PA.

[12] Fetkovich M.J. “The isochronal testing of oil wells.” SPE Paper 4529 presented at the Fall Meeting of the Society of Petroleum Engineers of AIME , Las Vegas, NV, Sep. 30-Oct. 3, 1973. DOI: 10.2118/4529-MS

[13] Gould, T. L.: “Compositional Two-Phase Flow in Pipelines,” 1975. Paper SPE 5685 presented in the 50th Annual Fall Meeting of the Society of Petroleum Engineers of AIME, Dallas, TX, USA, 28 September 1975.

[14] Gould, T.L., Tek, M.R. and Katz, D.K. 1974. “Two-Phase Flow Through Vertical, Inclined, or Curved Pipe.” J Pet Technol: 915-926. SPE 4487-PA.

[15] Gray, H.E. 1974. “Vertical Flow Correlation in Gas Wells.” In User manual for API 14B, Subsurface controlled safety valve sizing computer program, Appendix B. Washington, DC: API.

[16] Hagedorn, A.R. and Brown, K.E. 1965. “Experimental Study of Pressure Gradients Occuring During Continuous Two-Phase Flow in Small-Diameter Vertical Conduits.” J Pet Technol: 475-484. SPE 940-PA.

[17] Hanikson, R.W., Thomas, L.K. and Philips, K.A.: “Predict natural gas properties”, Hydrocarbon Processing, April 1969, 106-108.

[18] Hasan, A. R. and Kabir, C. S.: “Modeling Changing Storage During a Shut-in Test,” Paper SPE 24717 Presented at the SPE Annual Technical Conference and Exhibition, Washington DC, October 4-7 1992.

[19] Hasan, A. R., and Kabir, C. S.: “A Study of Multiphase Flow Behavior in Vertical Wells,” SPE Production Engineering Journal, May 1988, 263–272.

[20] Kabir, C.S. and A.R. Hasan: “Two-Phase Flow Correlations as Applied to Pumping Well Testing,” ASME J. of Energy Resources Tech., Vol. 116, 121-127 (June 1994). October.

[21] L.K., Thomas, Hankinson R.W., and Phillips K.A. “Determination of Acoustic Velocities for Natural Gases.” J. Pet. Tech. (1970): 889-895. Print.

[22] McCoy, J.N. “Measuring Liquid via Acoustic Velocity.” Pet. Engr.. (1975): n. page. Print.

[23] McCoy, J.N., A.L. Podio, K.L. Huddleston, and B. Drake. “Acoustic Statuc Bottomhole Pressures.” SPE 13810. (1985): n. page. Print.

[24] Mukherjee, H. and Brill, J.P.: “Liquid Holdup Correlations for Inclined Two-Phase Flow,” Journal of Petroleum Technology, pp. 1003-1008, May 1983.

[25] Orkiszewski, J. 1967. “Predicting Two-Phase Pressure Drops in Vertical Pipe.” J Pet Technol: 829-938. SPE 1546-PA.

[26] Petroleum Experts 2010. User Manual for IPM Prosper, version 12.0 and OpenServer.

[27] Podio, A.L.: Tarrillion, ML, and Roberts, E.T.: “Laboratory Work Improves Calculations,” pit & Gas J., Aug. 25, 1980, 137-46.

[28] Production Technology II Book, Heriot Watt University, 2010.

[29] Qasem, F. H, Nashavi, I. S., Mir, M. I.: “Detection of Pressure Buildup Data Dominated by Wellbore Phase Redistribution Effects,” Journal of Petroleum Science and Engineering, 2002, 34, 109-122.

[30] Qasem, F. H., Nashawi, I. S. and Mir, M. I.: “A New Method for the Detection of Wellbore Phase Redistribution Effects During Pressure Transient Analysis,” SPE 67239, Oklahoma, 24-27 March 2001.

[31] Rowlan, O. Lynn, and James N. McCoy. “Acoustic Determination of Fluid Level Measurement.” Gas Well Deliquification Workshop. Denver, Colorado. 02 Mar 2011. Speech.

[32] Sam, G., M. Kaestenbauer, Chr. Burgstaller, and E. Chevelcha. “Fully automated Fluid Level Measurement Tool.” SPE 145434. (2011).

[33] Shi, H., Holmes, J. A., Diaz, L. R., Durlofsky, L. J., and Aziz, K.: “Drift-Flux Parameters for Three-Phase Steady-State Flow in Wellbores,” Society of Petroleum Journal, June 2005, 130-137.

[34] Time, R.W. 2009. “Two-Phase Flow in Pipelines.” Course compendium, University of Stavanger.

[35] Vogel J.V.: “Inflow Performance Relationships for Solution-Gas Drive Wells,” JPTQw. 1968, 83-87; Trans., AIME, 243.

[36] Well Analyzer And TWM Software, Operating Manual, Echometer Company.

[37] Yahaya, A.U. and Gahtani, A.A. 2010. “A Comparative Study Between Empirical Correlations & Mechanistic Models of Vertical Multiphase Flow.” SPE 139631 ,Saudi Arabia, 04-07 April.

[38] Zavareh, F., Hill, A.D. and Podio, A.L. 1988. “Flow Regimes in Vertical and Inclined Oil/Water Flow in Pipes.” Paper SPE 18215, Houston, Texas, 02-05 October.

APPENDIX A-1: Completion sketch of V-043 Well

Komplettierung

der SONDE: **V-043**

Datum: 09-Dec-09

Ergänzungen:

Aussteller: *H. Österreicher*

Ergänzungen:

Voitsdorf 43

SH = 427,2m

T-Block: 3 1/8", 5 M
Flansch: 11", 5 M

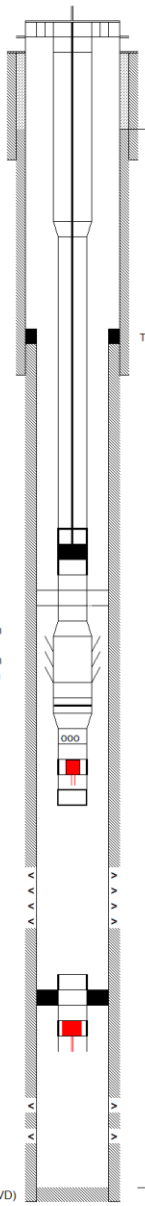

Einbaudaten	Länge: [m]	eingebaut (bzw.Teufe) bis [m]
10" x 12" x 3 1/2" EU Tubinghänger	0.24	0.24
3 1/2" EU Doppelnippel	0.18	0.42
86 Single 3 1/2" EU Tubing, 9,3 lb/ft	786.57	786.99
Übergang 3 1/2" EU M x 2 7/8" EU Z	0.28	787.27
102 Single 2 7/8" EU Tbg, 6,5 lb/ft, J-55	973.11	1760.38

Pumpenbock:	C-640 D 356 - 144	**Gewichte:**	2 x ORO	
Hubhöhe:	223 cm	**Pos. Gew.:**		
Hubzahl:	3,5 Hf/min	**Dyn. Spiegel:**		
Motor:	30 kW	**Rate theoret.:**		
Rotation:	gegen Uhrz. (Sonde rechts)	**Wirkung:**		

Details/Stk.		Ersteinbau am	Länge	kum. Länge
	1 1/2" x 30 ft Polierstange	10/27/2008	6.00	6.00
2 Kurzstk.	0,51 - 1,80 m	10/27/2008	2.31	8.31
112 Single	1" x 25 ft	10/27/2008	852.50	860.81
92 Single	7/8" x 25 ft	10/27/2008	701.04	1561.85
26 Single	1" x 25 ft	10/27/2008	197.12	1758.97
1 Single	7/8" x 25 ft	10/27/2008	7.62	1766.59
	2 1/4" Kolben 1,61 m/Fußv. 0,41m	10/27/2008	1.60	1768.19

2 7/8" EU Kurzstück	0.98	1761.36
Tubingpumpe 2 7/8" x 2 1/4" x 24 ft THC, mit ziehbarem FV	7.64	1769.00
2 7/8" EU Kurzstück	0.78	1769.78
7" Tubing Anchor Catcher	0.71	1770.49
2 7/8" EU Kurzstück	2.93	1773.42
Übergang 2 7/8" EUM x 3 1/2" EUZ	0.23	1773.65
3 1/2" EU Gasanker	3.00	1776.65
1 Single 3 1/2" EU Tubing, J-55, 9,3 lb/ft	9.05	1785.70
		1785.70
Übergang 3 1/2"EU M x 2 7/8"EU Z (gesschlossen)	0.27	1785.97
2 7/8" EU perforiertes KS	2.03	1788.00
2 7/8" EU KS	0.98	1788.98
2 7/8" EU X-Nipple (mit offenem Plug und Messgeräten)	0.28	1789.26
1 Single 2 7/8" EU Tbg, 6,5 lb/ft, J55	9.53	1798.79
2 7/8" EU ON/OFF Tool Oberteil	0.57	**1799.36**
2 7/8" EU ON/OFF Tool Unterteil	0.56	2148.60
7" G77 Hydraulikpacker	1.68	2150.28
1 Single 2 7/8" EU Tbg, J55, 6,5 lb/ft	9.54	2159.82
2 7/8" EU X-Landing Nipple (mit Plug und Messgeräten)	0.28	2160.10
1 Single 2 7/8" EU Tbg, J55, 6,5 lb/ft	9.54	2169.64
Zementsohle bei 2310 m (am 23.04.2008 getastet)		

Steigrohrgewicht , [to]: **21 to** (↑ 23 to / ↓ 20 to)
Gestängegewicht, [to]: **7,5 to**

Abstreiffestigkeit Tbg.: 100%
45,2 to für 2 7/8"
64,6 to für 3 1/2"

Absetzdaten: Last, [to]:
Spannung, [to]: **5**

Anker lösen:

EINBAUTEN					
Tubing			**Pumpgestänge**		
2 3/8" EU		Stk.	3/4" x 25 ft		Stk.
2 7/8" EU	105	Stk.	7/8" x 25 ft	93	Stk.
3 1/2" EU		Stk.Poly	1" x 25 ft	138	Stk.
3 1/2" EU	87	Stk.	1 1/8" x 25 ft		Stk.
Summe	**192**	Stk.	Summe	**231**	Stk.

Investnummern:
Anker:
Packer:
Pumpe:

APPENDIX A-2: Completion sketch of BH-003 Well

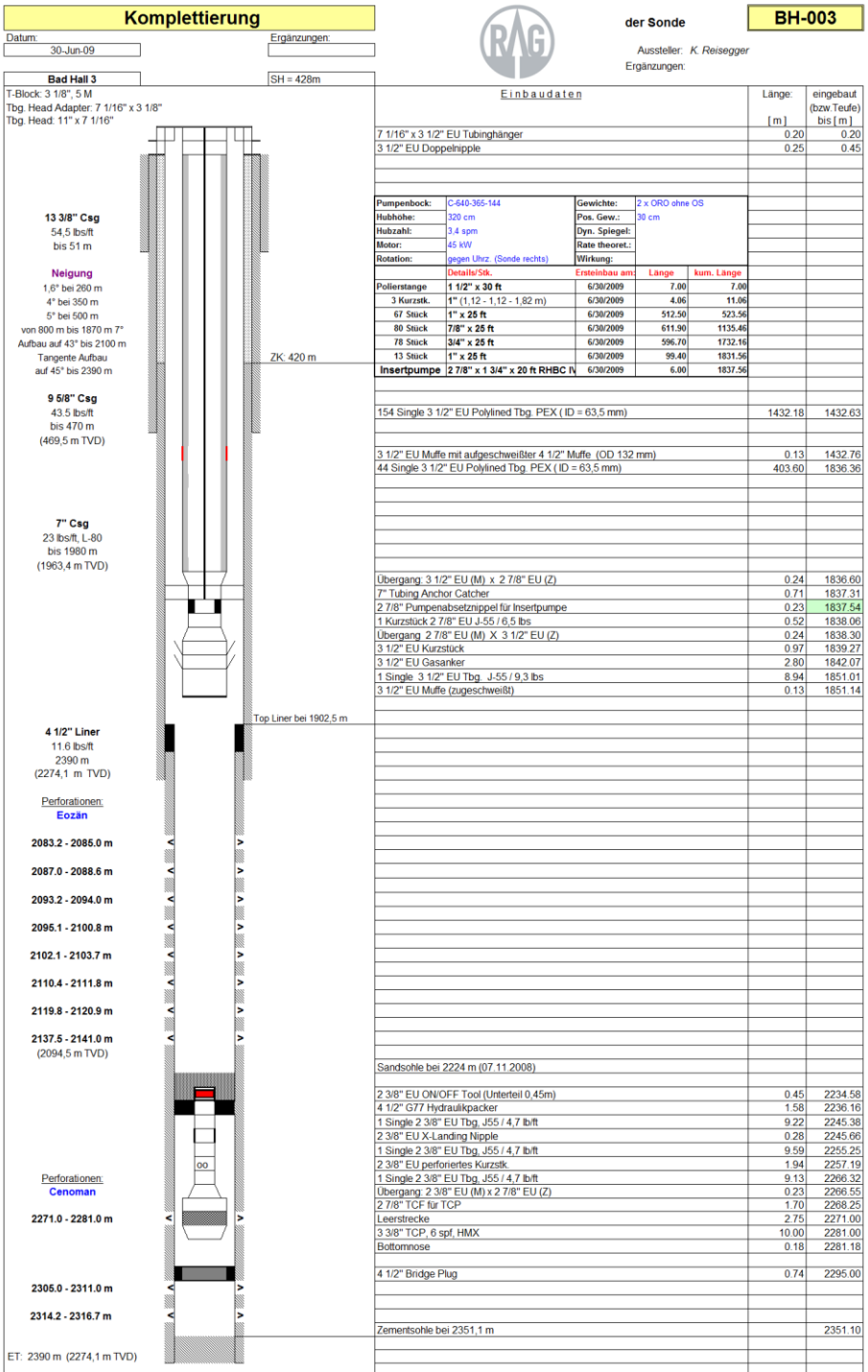

APPENDIX B-1: The Procedure of pressure calculation at Steady State using Excel and Prosper method

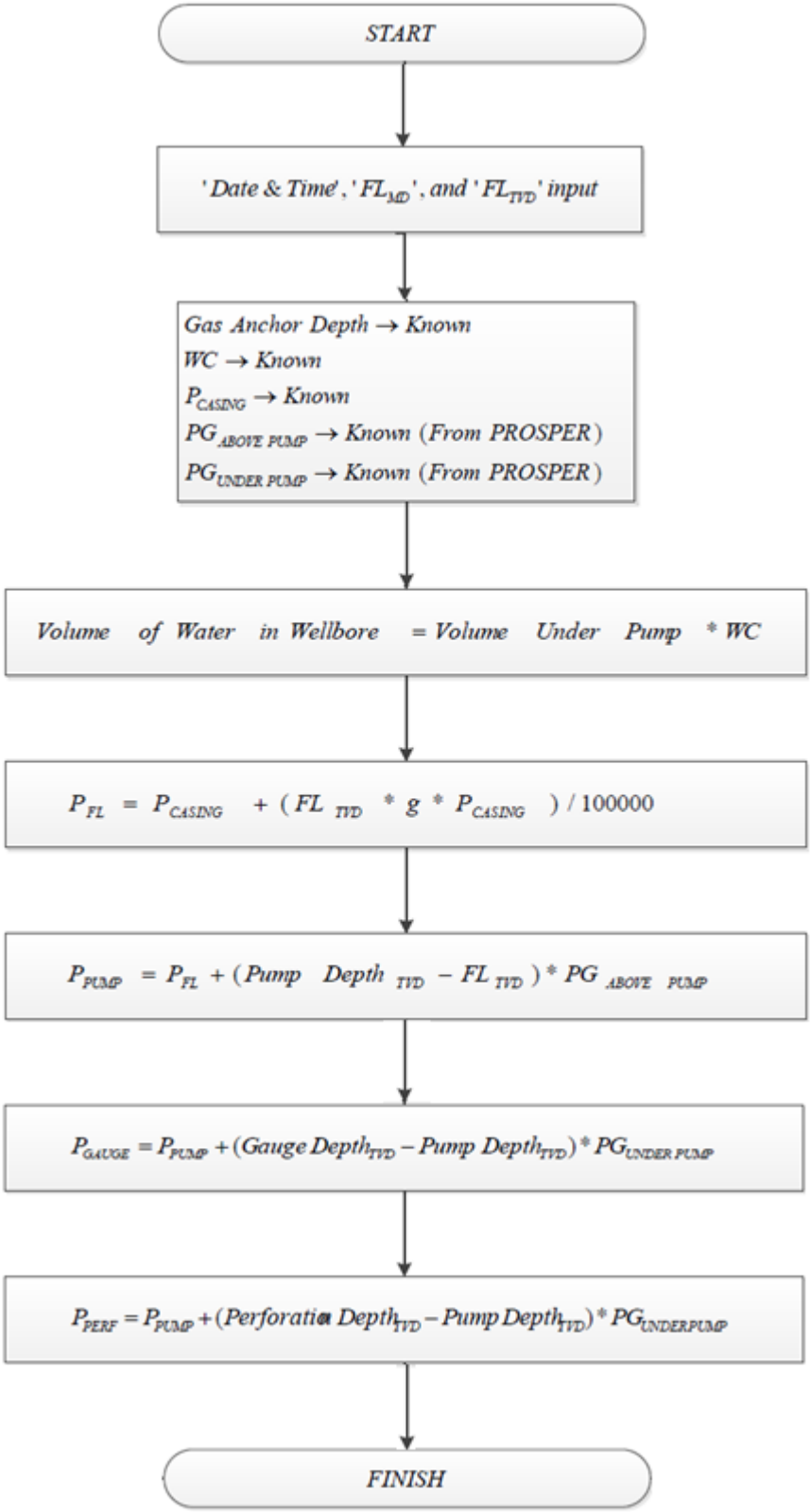

APPENDIX B-2: The Procedure of pressure calculation at Transient Condition using Excel and Prosper method

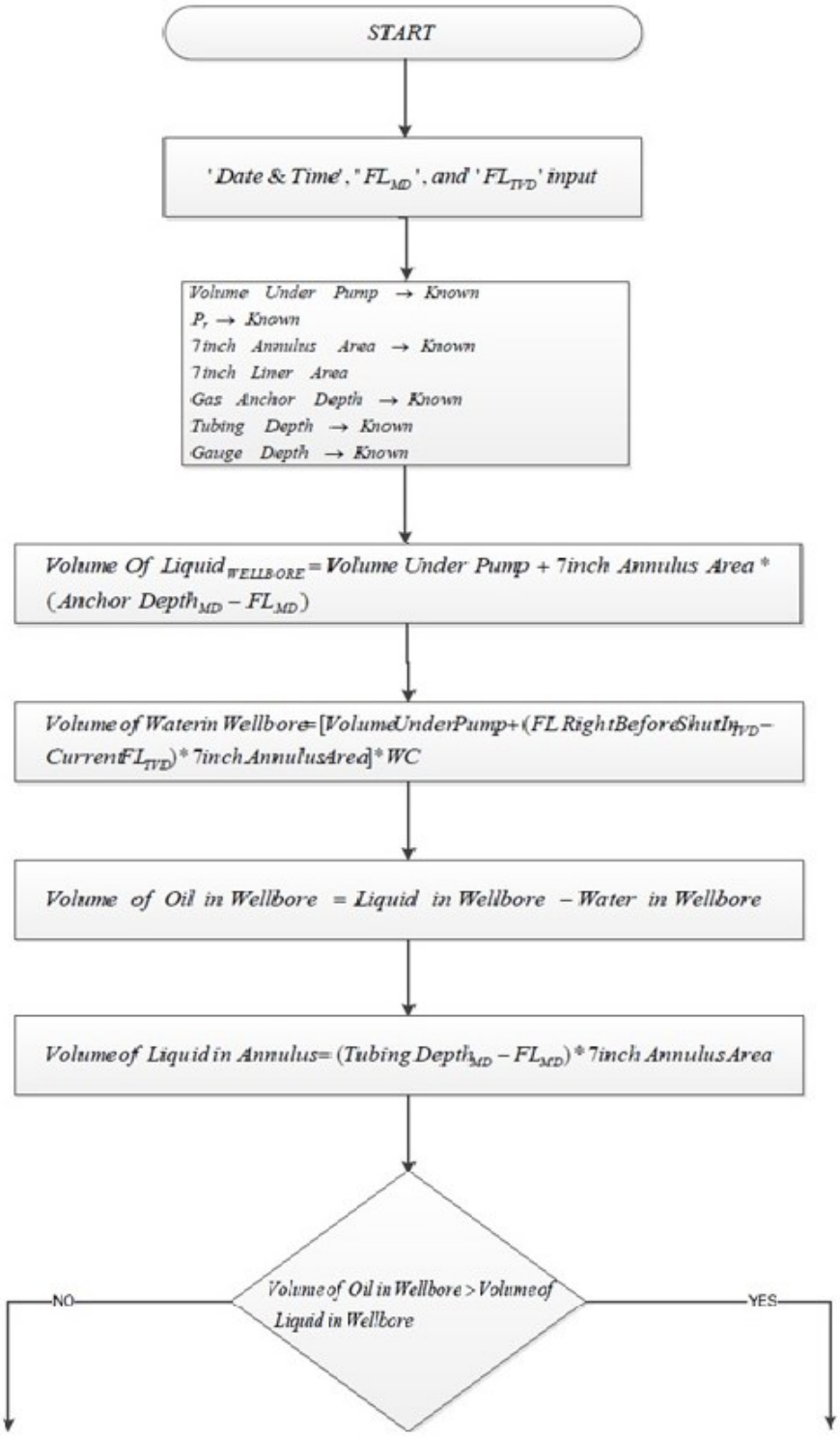

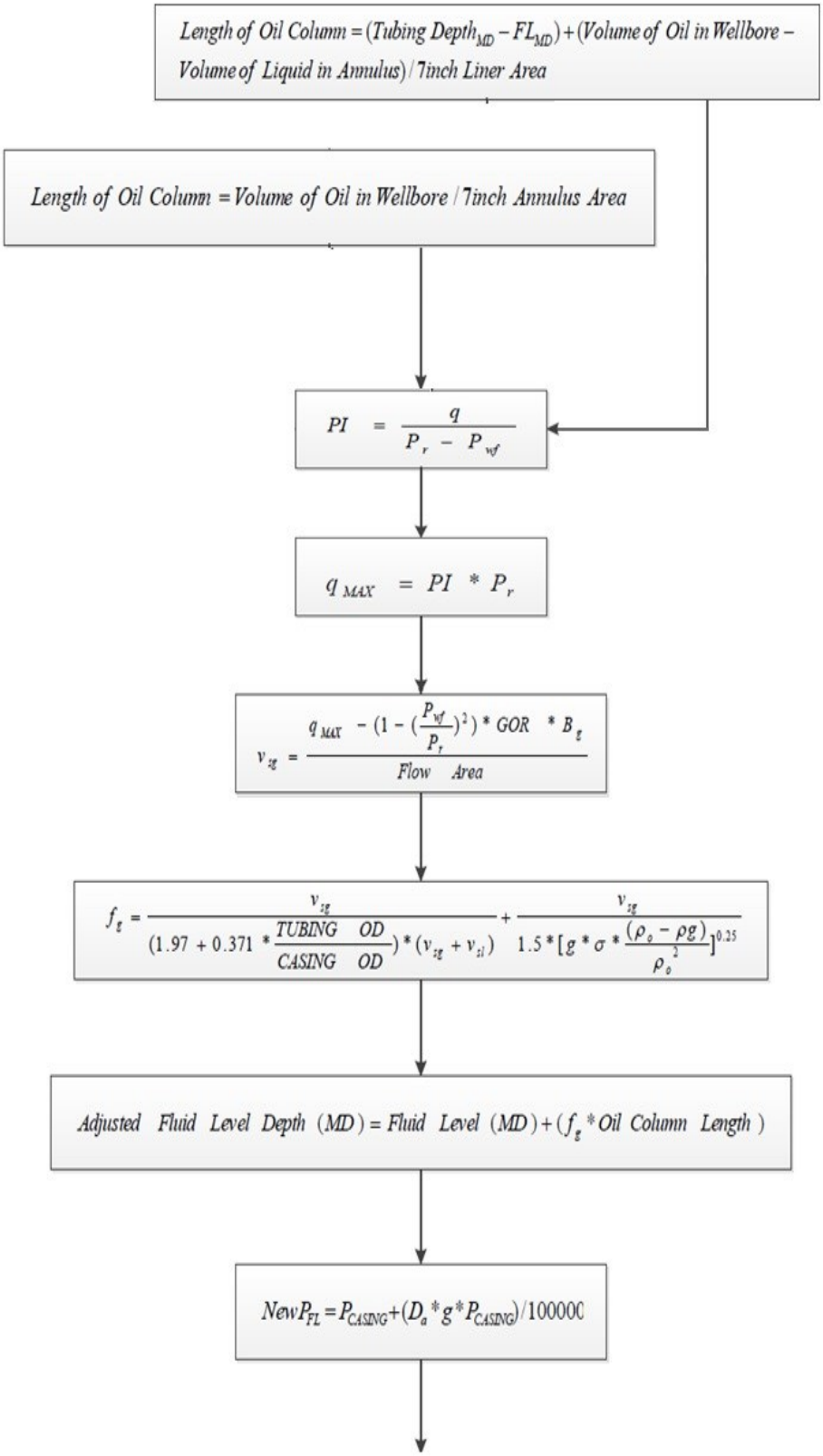
Length of Oil Column = (Tubing Depth$_{MD}$ – FL$_{MD}$) + (Volume of Oil in Wellbore – Volume of Liquid in Annulus) / 7inch Liner Area
Length of Oil Column = Volume of Oil in Wellbore / 7inch Annulus Area
$PI = \frac{q}{P_r - P_{wf}}$
$q_{MAX} = PI * P_r$
$v_{sg} = \frac{q_{MAX} - (1 - (\frac{P_{wf}}{P_r})^2) * GOR * B_g}{Flow\ Area}$
$f_g = \frac{v_{sg}}{(1.97 + 0.371 * \frac{TUBING\ OD}{CASING\ OD}) * (v_{sg} + v_{sl})} + \frac{v_{sg}}{1.5 * [g * \sigma * \frac{(\rho_o - \rho g)}{\rho_o^2}]^{0.25}}$
Adjusted Fluid Level Depth (MD) = Fluid Level (MD) + (f_g * Oil Column Length)
New$P_{FL} = P_{CASING} + (D_a * g * P_{CASING}) / 100000$

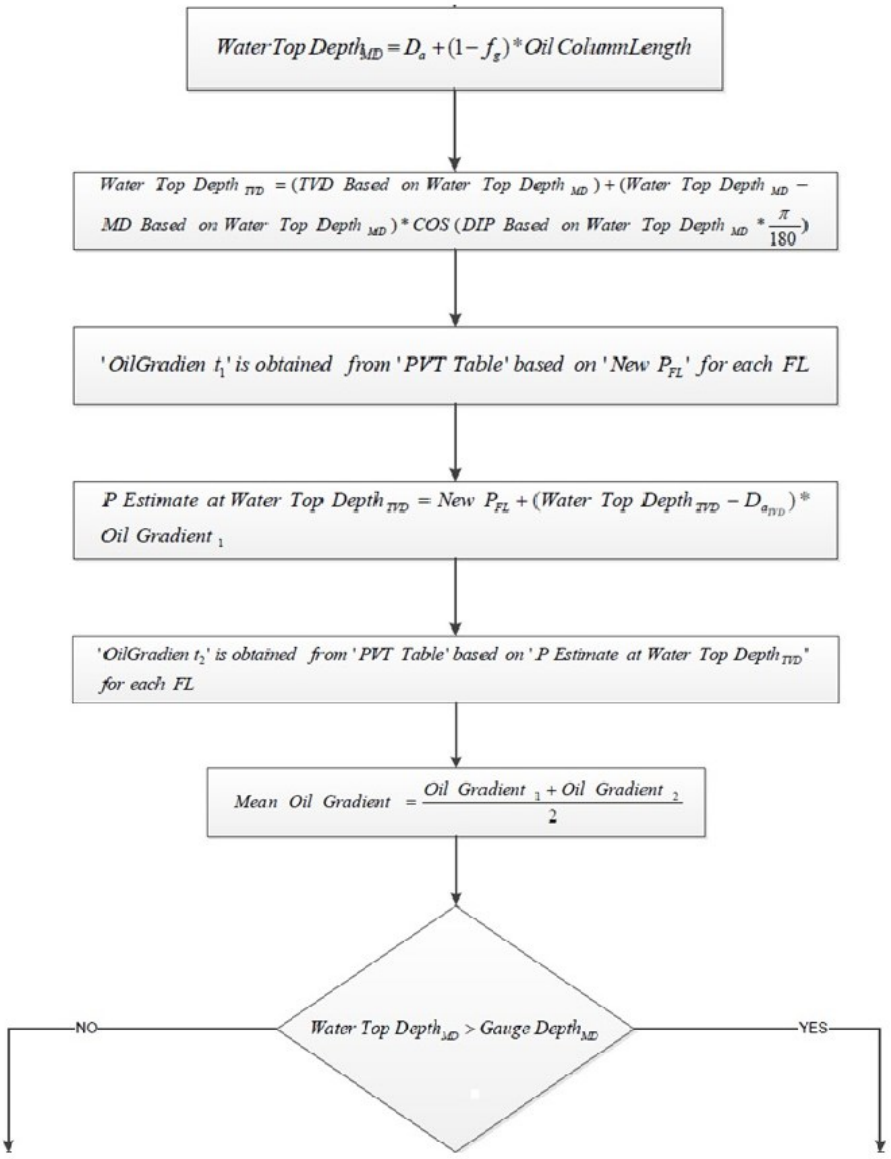
$Water\ Top\ Depth_{MD} = D_a + (1 - f_g) * Oil\ Column Length$
$Water\ Top\ Depth_{TVD} = (TVD\ Based\ on\ Water\ Top\ Depth_{MD}) + (Water\ Top\ Depth_{MD} - MD\ Based\ on\ Water\ Top\ Depth_{MD}) * COS(DIP\ Based\ on\ Water\ Top\ Depth_{MD} * \frac{\pi}{180})$
'OilGradien t_1' is obtained from 'PVT Table' based on 'New P_{FL}' for each FL
$P\ Estimate\ at\ Water\ Top\ Depth_{TVD} = New\ P_{FL} + (Water\ Top\ Depth_{TVD} - D_{a_{TVD}}) * Oil\ Gradient_1$
'OilGradien t_2' is obtained from 'PVT Table' based on '$P\ Estimate\ at\ Water\ Top\ Depth_{TVD}$' for each FL
$Mean\ Oil\ Gradient = \frac{Oil\ Gradient_1 + Oil\ Gradient_2}{2}$
$Water\ Top\ Depth_{MD} > Gauge\ Depth_{MD}$
NO
YES

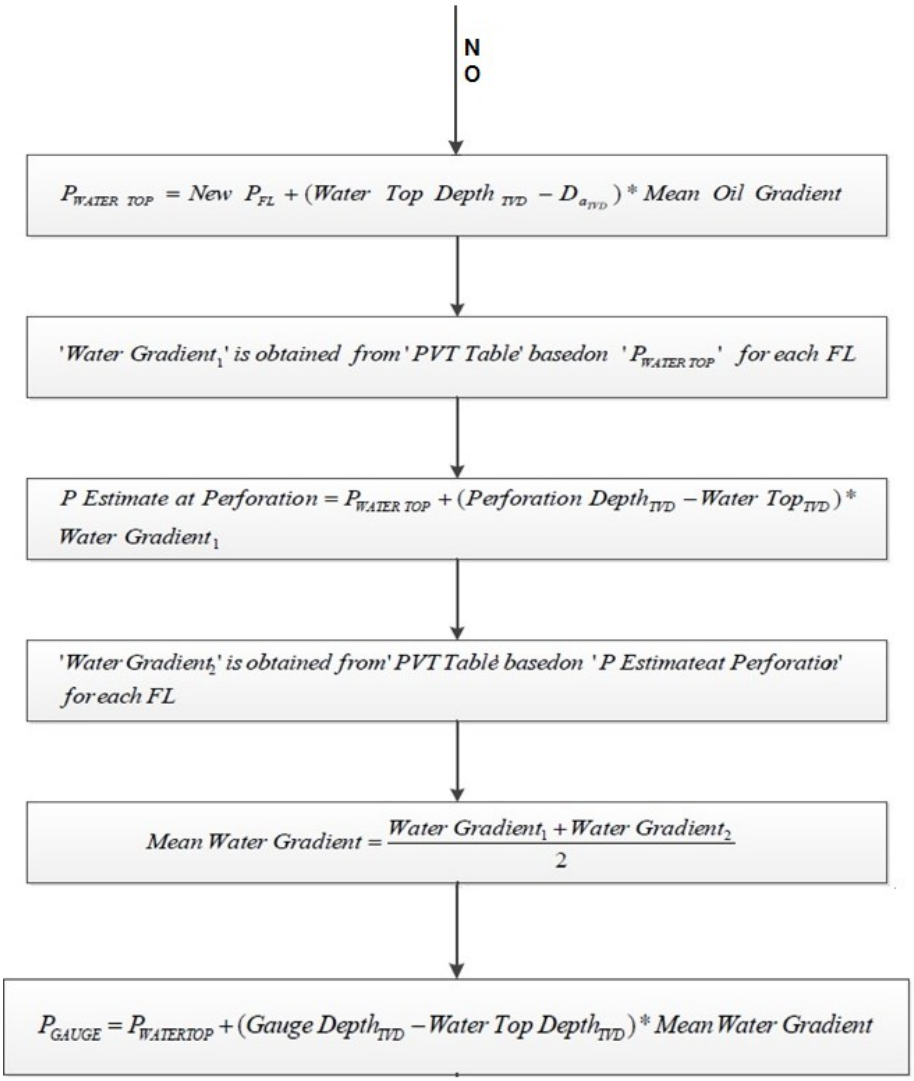
NO
$P_{WATER\ TOP} = New\ P_{FL} + (Water\ Top\ Depth_{TVD} - D_{a_{TVD}}) * Mean\ Oil\ Gradient$
'Water Gradient$_1$' is obtained from 'PVT Table' basedon 'P$_{WATER\ TOP}$' for each FL
P Estimate at Perforation = $P_{WATER\ TOP} + (Perforation\ Depth_{TVD} - Water\ Top_{TVD}) *$ Water Gradient$_1$
'Water Gradient$_2$' is obtained from 'PVT Table' basedon 'P Estimateat Perforation' for each FL
$Mean\ Water\ Gradient = \frac{Water\ Gradient_1 + Water\ Gradient_2}{2}$
$P_{GAUGE} = P_{WATERTOP} + (Gauge\ Depth_{TVD} - Water\ Top\ Depth_{TVD}) * Mean\ Water\ Gradient$

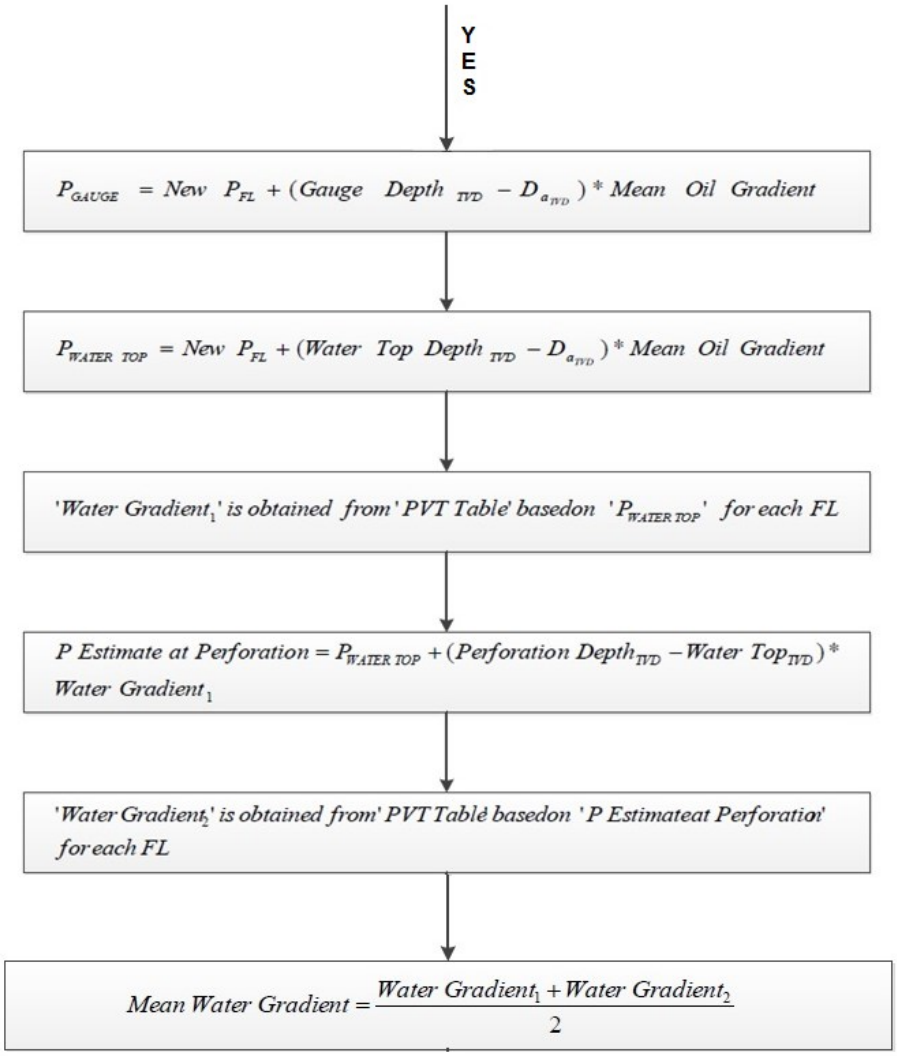
YES
$P_{GAUGE} = New\ P_{FL} + (Gauge\ Depth_{TVD} - D_{a_{TVD}}) * Mean\ Oil\ Gradient$
$P_{WATER\ TOP} = New\ P_{FL} + (Water\ Top\ Depth_{TVD} - D_{a_{TVD}}) * Mean\ Oil\ Gradient$
'Water Gradient$_1$' is obtained from 'PVT Table' basedon '$P_{WATER\ TOP}$' for each FL
P Estimate at Perforation = $P_{WATER\ TOP} + (Perforation\ Depth_{TVD} - Water\ Top_{TVD}) *$ Water Gradient$_1$
'Water Gradient$_2$' is obtained from 'PVT Table' basedon 'P Estimateat Perforation' for each FL
$Mean\ Water\ Gradient = \frac{Water\ Gradient_1 + Water\ Gradient_2}{2}$

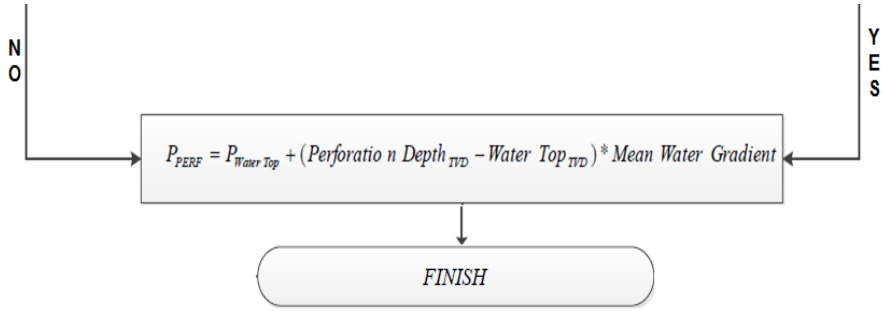
NO
YES
$P_{PERF} = P_{Water\ Top} + (Perforation\ Depth_{TVD} - Water\ Top_{TVD}) * Mean\ Water\ Gradient$
FINISH

APPENDIX C-1: The Procedure of pressure calculation at Steady State using VB-Script and Prosper method

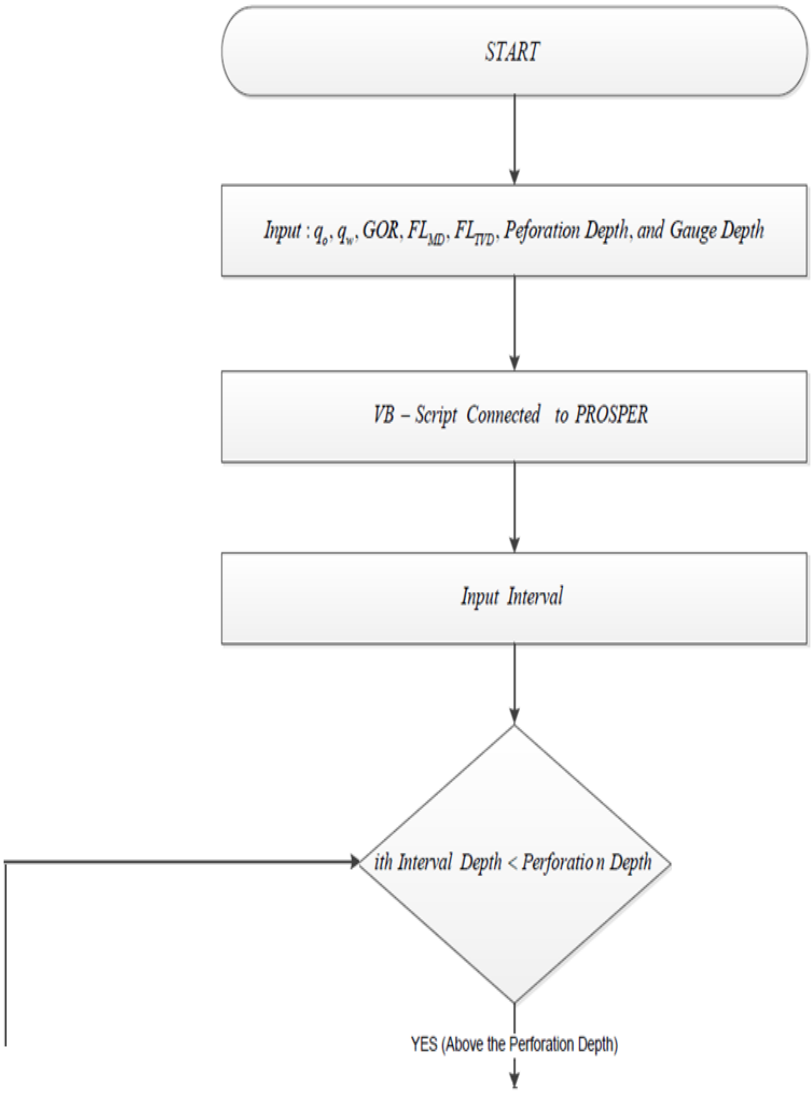

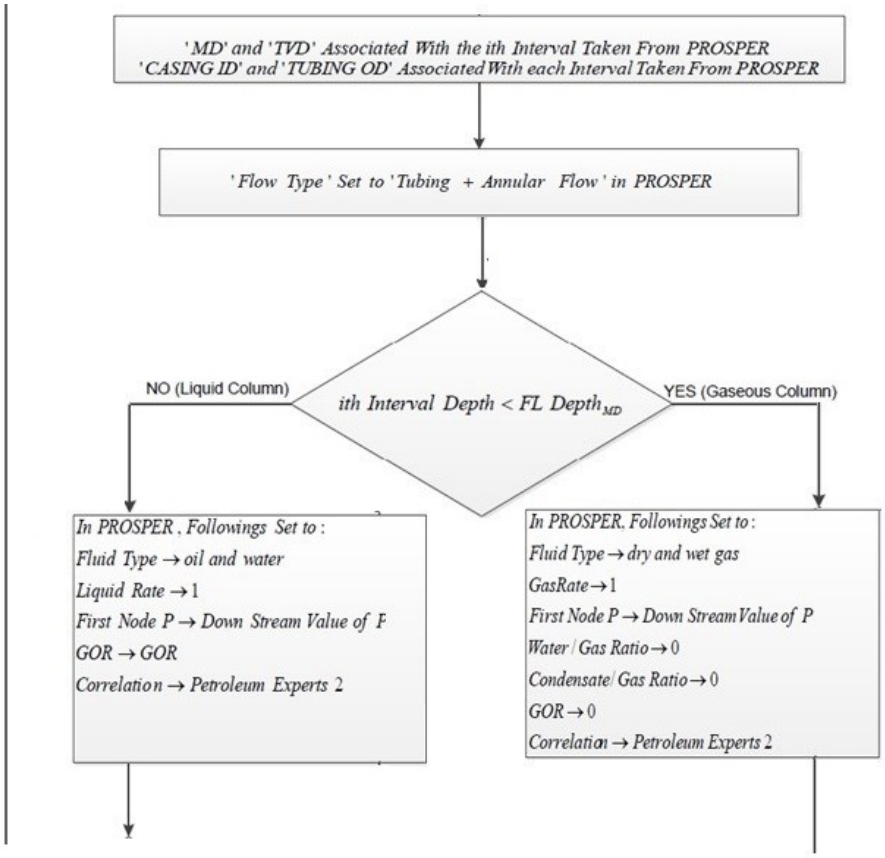
'MD' and 'TVD' Associated With the ith Interval Taken From PROSPER
'CASING ID' and 'TUBING OD' Associated With each Interval Taken From PROSPER
'Flow Type' Set to 'Tubing + Annular Flow' in PROSPER
NO (Liquid Column)
ith Interval Depth < FL Depth MD
YES (Gaseous Column)
In PROSPER, Followings Set to:
Fluid Type → oil and water
Liquid Rate → 1
First Node P → Down Stream Value of P
GOR → GOR
Correlation → Petroleum Experts 2
In PROSPER, Followings Set to:
Fluid Type → dry and wet gas
GasRate → 1
First Node P → Down Stream Value of P
Water / Gas Ratio → 0
Condensate/ Gas Ratio → 0
GOR → 0
Correlation → Petroleum Experts 2

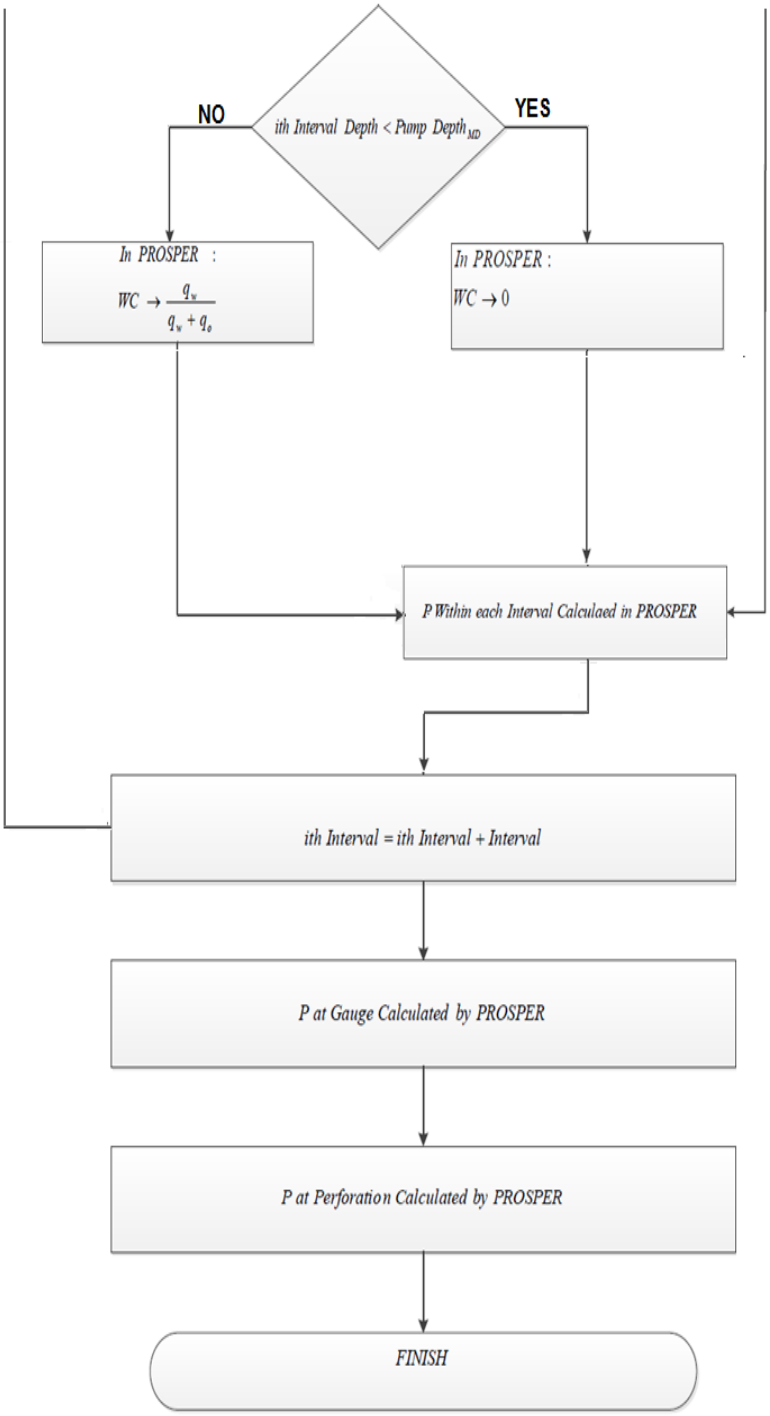
ith Interval Depth < Pump Depth MD
NO
YES
In PROSPER :
WC → q_w / (q_w + q_o)
In PROSPER :
WC → 0
P Within each Interval Calculaed in PROSPER
ith Interval = ith Interval + Interval
P at Gauge Calculated by PROSPER
P at Perforation Calculated by PROSPER
FINISH

APPENDIX C-2: The Procedure of pressure calculation at Transient Condition using VB-Script and Prosper method

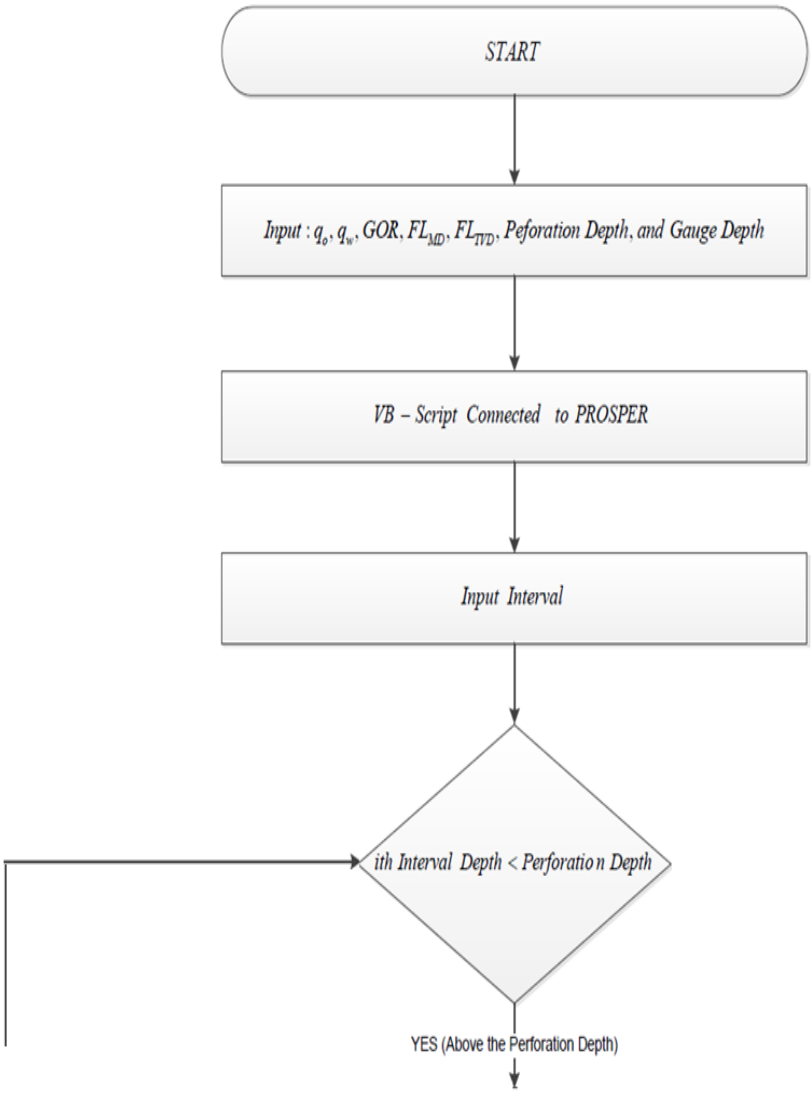

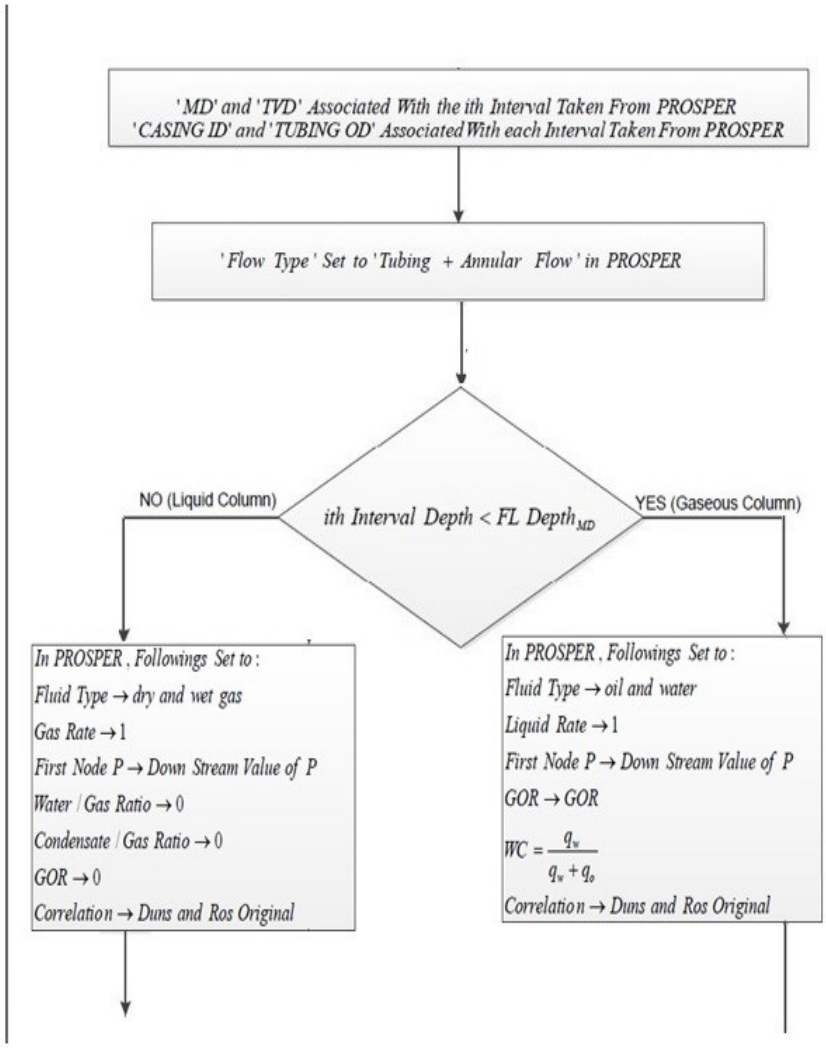
'MD' and 'TVD' Associated With the ith Interval Taken From PROSPER
'CASING ID' and 'TUBING OD' Associated With each Interval Taken From PROSPER
'Flow Type' Set to 'Tubing + Annular Flow' in PROSPER
NO (Liquid Column)
ith Interval Depth < FL Depth MD
YES (Gaseous Column)
In PROSPER, Followings Set to:
Fluid Type → dry and wet gas
Gas Rate → 1
First Node P → Down Stream Value of P
Water / Gas Ratio → 0
Condensate / Gas Ratio → 0
GOR → 0
Correlation → Duns and Ros Original
In PROSPER, Followings Set to:
Fluid Type → oil and water
Liquid Rate → 1
First Node P → Down Stream Value of P
GOR → GOR
WC = qw / (qw + qo)
Correlation → Duns and Ros Original

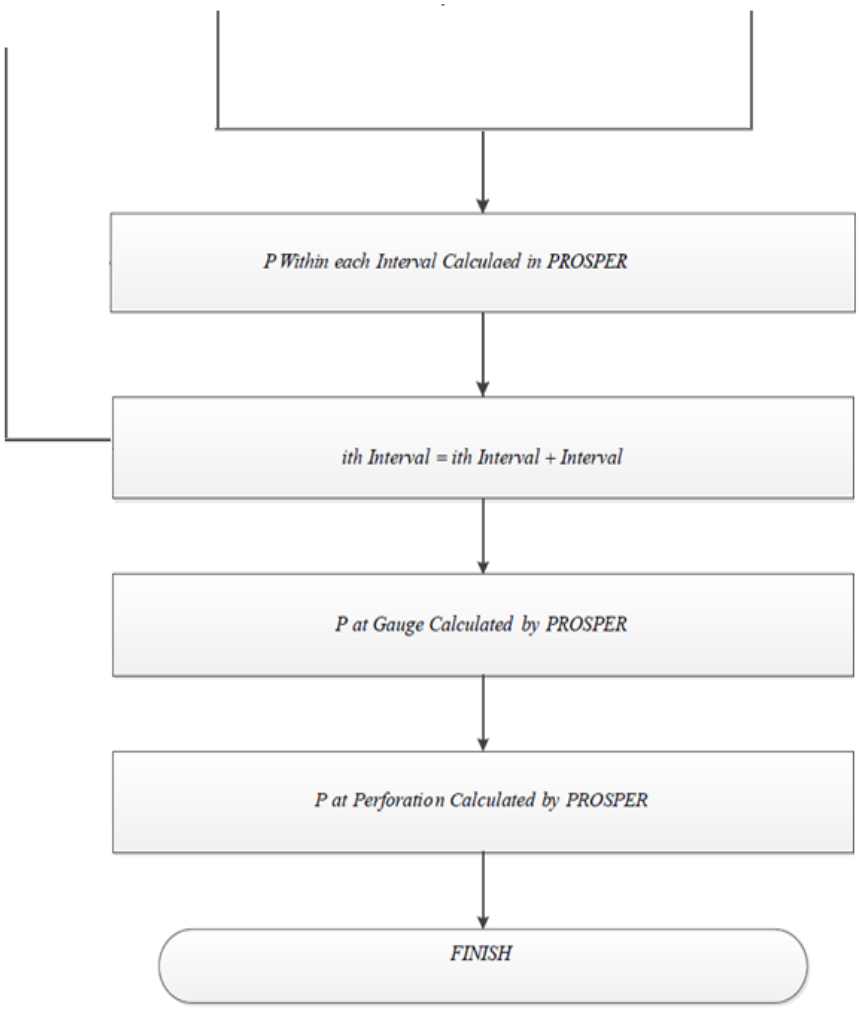
P Within each Interval Calculaed in PROSPER
ith Interval = ith Interval + Interval
P at Gauge Calculated by PROSPER
P at Perforation Calculated by PROSPER
FINISH